2-1-2019

Integrated fast optical modulators

Mohamed Youssef Abdelatty

Integrated Fast Optical Modulators

by
Mohamed Youssef Abdelatty
#800140201

Under the supervision of
Associate Prof. Mohamed Abdel Azim Swillam

A thesis submitted in conformity with the requirements
for the degree of « Physics (M.Sc.) »

« Department of Physics »
« School of Sciences and Engineering »
The American University in Cairo

The American University in Cairo
« School of Sciences and Engineering »
« Department of Physics »

« Integrated Fast Optical Modulators »

by
« Mohamed Youssef Abdelatty »
Submitted to
« Department of Physics »
In Partial Fulfillment of the requirements for
The Degree of Master of Science

EXAMINERS COMMITTEE

Name	**Signature**
Dr. Mohamed Swillam (Advisor) Associate Professor, Physics Department, AUC	_____ Date:_____
Dr. Salah El-Sheikh (Internal Examiner) Professor, Physics Department, AUC	_____ Date:_____
Dr. Hamdy Abdel Hamid (External Examiner) Associate Professor, Zewail City of Science and Technology	_____ Date:_____
Dr. Nageh Allam (Moderator) Associate Professor, Physics Department, AUC	_____ Date:_____

Table of Contents

List of Figures

List of Tables

List of Equations

List of Abbreviations

Si	Silicon
SPP	surface plasmon polariton
EOM	electro-optical modulator
α	photo-absorption coefficient
EAM	Elecro-absorption Modulator
WG	waveguide
DC	Directional coupler
VO_2	Vanadium dioxide
EO	Electro-optical
EA	Electro-absorption
ER	Extinction Ratio
IL	Insertion loss
FOM	Figure-of-merit
CPU	central-processing-unit
MZI	Mach–Zehnder interferometer
MOS	metal-oxide-semiconductors
WG	waveguide
ENZ	epsilon-near-zero
TCO	Transparent conducting oxide
ITO	Indium-tin-oxide

List of Publications[1]

[A] **M. Y. Abdelatty**, A. O. Zaki, and M. A. Swillam, "Hybrid silicon organic directional coupler based modulator," presented at the *META'16, the 7th International Conference on Metamaterials, Photonic Crystals and Plasmonics*, Malaga, Spain, 2016, pp. 440–441.

[B] **M. Y. Abdelatty**, A. O. Zaki, and M. A. Swillam, "Hybrid silicon plasmonic organic directional coupler-based modulator," *Appl. Phys. A*, vol. 123, no. 1, p. 11, Jan. 2017.

[C] **M. Abdelatty**, M. Abdelatty, M. M. Badr, and M. A. Swillam, "Hybrid Plasmonic Electro-Optical Directional Coupler Based Modulator Based on Electrically Tuning the ITO's Properties," in *Frontiers in Optics 2017, paper JW4A.43*, 2017, p. JW4A.43.

[D] **M. Y. Abdelatty**, M. M. Badr, and M. A. Swillam, "Hybrid plasmonic electro-optical absorption modulator based on epsilon-near-zero characteristics of ITO," in *Integrated Optics: Devices, Materials, and Technologies XXII*, 2018, vol. 10535, p. 105351T.

Under submission

[E] **M. Abdelatty**, M. M. Badr, and M. A. Swillam, "Hybrid Plasmonic Electro-Optical Directional Coupler Based Modulator Based on Electrically Tuning the ITO's Properties," Submitted to J. Light. Technol. (JLT).

[F] **M. Y. Abdelatty**, M. M. Badr, and M. A. Swillam, "Hybrid plasmonic electro-optical absorption modulator based on epsilon-near-zero characteristics of ITO," Submitted to J. Nanophotonics (JNP).

[G] **M. Y. Abdelatty**, M. M. Badr, and M. A. Swillam, "Hybrid plasmonic-vanadium dioxide electro-optical switch based modulator," Submitted to META'18, the 9th International Conference on Metamaterials, Photonic Crystals and Plasmonics.

[H] **M. Y. Abdelatty**, M. M. ElGarf, and M. A. Swillam, "Hybrid Vanadium Dioxide Plasmonic Electro-Optical Modulator based on Race-Track shaped Resonator," Submitted to *Frontiers in Optics 2018*.

Co-Authored

[I] M. Badr, **M. Abdelatty**, M. Abdelatty, and M. A. Swillam, "All-Silicon Directional Coupler Electro-Optic Modulator Utilizing Transparent Conducting Oxides," in Frontiers in Optics 2017 (2017), paper JW4A.41, 2017, p. JW4A.41.

[J] M. M. Badr, **M. Y. Abdelatty**, and M. A. Swillam, "All-silicon transparent conducting oxide-integrated electro-optical modulator," in Integrated Optics: Devices, Materials, and Technologies XXII, 2018, vol. 10535, p. 1053520.

[K] M. Badr, **M. Abdelatty**, M. Abdelatty, and M. A. Swillam, "All-Silicon Directional Coupler Electro-Optic Modulator Utilizing Transparent Conducting Oxides," Submitted to J. Photon. Technol. Lett. (PTL).

[1] (underlined = presenter)

Abstract

Over the past two decades, the demand for network interconnects, for both communication systems and intra/on-chip data links, increased in terms of capacities and bandwidth. To transmit digital signal over an optical traveling wave, the optical wave should be modulated using the digital electronic signal. An electro-optical modulator is responsible for switching the optical wave to pass or block it depending on the information digital signal. Such modulators are the key components in any optical communication system, since they convert the digital electronic signals to optical signals to travel over the optical fibers for long distances with minor losses. On chip level, copper interconnects are the bottleneck for the next generation technology because of their losses, dispersion, and speed. This has paved the way for replacing them with optical interconnects. Electro-optical modulators are the workhorses of such interconnects.

To achieve the goal of replacing electrical interconnects with optical ones, a high level of integration should be accomplished. This can be only achieved by combining both optical and electrical components on the same substrate. Thus, silicon photonics is being a prominent candidate for this technology because of its low cost, and CMOS compatibility.

Silicon as active material for optical modulation has a lot of limitations such as weak electro-optic effects and slow response of plasma dispersion effect. This raised the necessity for studying other novel alternative materials such as organic polymers, indium-tin-oxide (ITO), and vanadium dioxide.

In this dissertation, novel electro-optical modulators, based on different active materials and different structures, are proposed. The main concern in these designs is the compatibility with the wide spread silicon CMOS technology. These modulators rely on the plasmonic theory to confine light beyond the diffraction limit.

We introduce four high performance electro-optical modulators that operates under the telecommunication wavelength (1550 nm).

An organic hybrid-plasmonic optical directional coupler is designed and studied. The power-splitting mechanism based on the change of the polymer electro-optical characteristics upon applying an external electric field. A finite element method with a perfect matching layer used to simulate this design. An extinction ratio of 14.34 dB is achieved for 39 μm modulation length.

Two hybrid silicon electro-optical modulators are introduced and analyzed. The active material for these designs is Indium-Tin-Oxide. The first is based on tri-coupled waveguides with electrical tuning mechanism that is designed to change both the coupling conditions and introduces additional intrinsic losses. Based on this design, extinction ratio of 6.14dB and insertion losses of 0.06 dB are realized at 21 μm modulator length; as well as, extinction ratio of 11.43 dB and insertion losses of 1.65 dB are realized at 34 μm modulator length. The second device is an electro-absorption modulator, based on dielectric slot waveguide with an ITO plasmonic modulation section. An extinction ratio of 15.49 dB and an insertion loss of 1.01 dB can be achieved for 10 μm long modulation section. Modal and finite difference time domain analysis were performed to verify and simulate both designs.

Last but not least, an optical switch based on a hybrid plasmonic-vanadium dioxide waveguide is presented. The power-attenuating mechanism takes the advantage of the phase change properties of vanadium dioxide that exhibits a change in the real and complex refractive indices upon switching from the dielectric phase to the metallic phase. An extinction ratio per unit length of 4.32 dB/μm and insertion loss per unit length of 0.88 dB/μm are realized. Also, Modal and finite difference time domain analysis are taken up to study and optimize this design.

The proposed silicon electro-optical modulators can potentially play a key role in the next generation of the on-chip electronic-photonic integrated circuits.

Dedication

This thesis is dedicated to my parents, who have continuously loved me and whose good models taught perseverance in achieving my goals. I would not be where I am, now, without their unconditional support and love. Also, I want to thank my sisters whom I am very thankful to have them in my life. This work is, also, dedicated to my best friends who have been a constant source of encouragement and support during my masters years.

Mohamed Y. Abdelatty

Acknowledgments

First and foremost, I would like to thank my thesis advisor, Prof. Mohamed Swillam, for encouraging and guiding me through my thesis and graduate studies. I am grateful for his ideas that sparkled my mind and made me passionate about my thesis topic. Also, I am very thankful for our long discussions, which he managed to arrange although his busy schedule.

Also, I would like to thank the past and current students and colleagues in our group, Nanophotonics Research Laboratory (NRL), for their tremendous advice and help.

I would also like to thank all of the British University in Egypt, Faculty of Engineering members who supported me and managed organizing my workload to fit in with my study timetable.

Last but not least, I would like to thank the members of my dissertation committee for generously offering their time.

Chapter 1 Introduction

Optical signals have a very long history. Smoke signals were used by ancient people to transmit messages from a mountain top to another mountain top. In ancient China, soldiers, along the great wall, signaled fire smoke to send alerts of enemy attacks from tower to tower [1], [2].

Since that time, many efforts exerted to develop optical communications systems. The challenge was to develop an information carrying channel, that is cheap, reliable, could be used for long distances at high data rate. This made possible by the total internal reflection. This phenomenon makes light reflect, rather than refract, when attempting to pass from transparent optical medium to a less optical density medium. In 1854, John Tyndall showed the guidance of light inside a transparent medium with an optical density discontinuity at boundaries [3], [4].

Optical fibers use total internal reflection phenomenon to keep light trapped inside the denser glass, the core. Optical fibers have two main advantages. they are costly effective and have low attenuation.

Nowadays, an optical fiber cable is made of a hair-thin strands of plastic or glass, known as optical fibers. One optical fiber cable can have as many as several hundreds of strands. Each strand can carry about 25,000 calls; an entire cable can carry several million calls [5].

1.1 The role of modulators in optical communication systems

Over the past two decades, the demand increased for telecommunication network capacities and bandwidth. For example, in carrier networks, data traffic increases at a rate of 60% per year [6]. Also, the rising cloud-based computing is expected to increase the machine-to-machine data traffic by 90% per year [6]. Cisco forecasts data traffic to be 20.6 zettabytes per year by the year of 2021 [7].

To fit with these growing bandwidth demand, electronic baseband systems are replaced by optical broadband systems. Optical communication systems have many advantages, such as low cost, high bandwidth, low transmission losses for long distances. To transmit digital electronic signal over optical traveling wave, the optical wave should be modulated using the electronic signal.

The simplest optical modulation scheme is the Direct Laser Modulation, which is based on directly controlling the drive current to change the intensity of the output optical wave. This technique has many drawbacks like the bandwidth and extension ratio limitations, and signal distortion due to frequency chirping [8].

The second scheme is the external modulation, where a continuous wave laser is used to emit optical wave and the modulation is done by an external modulator. The modulator is responsible for switching the optical wave to pass or block it depending on the information signal [8]. A general model of optical communication (transmitter/receiver) system with external modulator is depicted in Figure 1.1. A modulator is a key component in any optical communication systems; it's role is very similar to that of a transistor in electronic circuits [6].

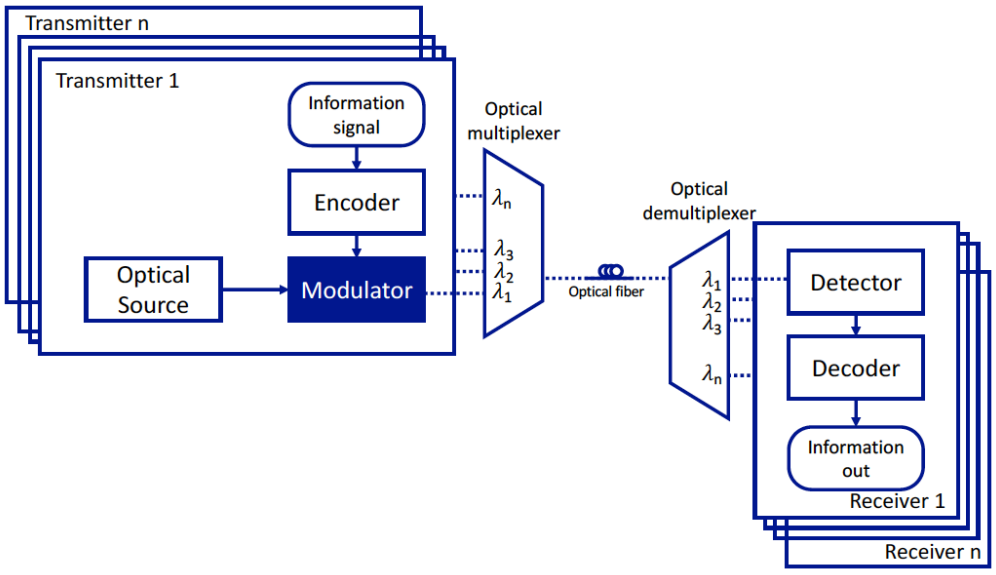

Figure 1.1 - A schematic of A general model of optical communication (transmitter/receiver) system with external modulator.

Square blocks indicate the system components and the circular blocks indicate the system input and output signals.

Thus, the need to developing external modulators is increasing as the demand for optical communication systems is increasing. Modern optical communication systems are moving towards integrating dense optical modulators to reduce both the energy consumption and the cost.

1.2 The role of modulators as interconnects

The growing demand for high-capacity signal processing systems has increased over the past decades and has led to the miniaturization of transistors. Performance

limitations are mainly due to the electrical copper interconnects associated properties, such as RC delay, signal distortion, and power consumption [9], [10]. Replacing copper wiring with optical interconnect layer can transcend these limitations. Low signal distortion can be obtained at very high frequencies (>10GHs) and long distances (>1 cm). [10]

The prospect expansion in supercomputers will demand high bandwidth interconnects to connect central-processing-unit (CPU) to another, CPU to memory, and node to another node in the cluster [11]. The bandwidth limitations and the high power consumption of the electrical interconnects affect the operating speeds of the processors. High speed electro-optical modulators (EOMs) are the key components for the on-chip silicon photonic circuits since they interconnect the digital electronic and photonic worlds by modulating optical signals by electrical signals.

To achieve the goal of replacing electrical interconnects with optical ones, a high level of integration should be accomplished. This can be achieved only by using monolithic integration; all optical and electrical elements are incorporated on the same substrate. These elements include light sources, electro-optical modulators, and detectors. The material for such substrate, nowadays, is silicon (Si) [12].

1.3 Silicon photonics and plasmonics

During the same time that demand for optical communication systems increased, noteworthy development has happened in the field of silicon photonics. The material system used for electronic circuitries for many decades, now is used to build optical integrated devices and circuits. Silicon photonics is very appealing since it uses the existing CMOS-VLSI technology, and cheaper for mass production. Also, silicon is almost transparent at the telecommunication wavelengths.

So far, many Si EOMs have been developed based on carrier concentration change effect including, but not limited to, Mach–Zehnder interferometers (MZIs), ring resonators, and metal-oxide- semiconductor capacitors [13]–[18]. Although modulators based on MZIs are promising in terms of modulation speed and optical bandwidth, they suffer from the large device footprints. While modulators based ring resonators have very narrow bandwidth [19].

To overcome these drawbacks, different designs have been studied [16], [20]–[24]. Among these designs, modulators based on directional couplers attract the attention because of their relatively small sizes and high bandwidth [25], [26].

The minimum size offered by Silicon photonics to guide light efficiently is about 200 nm due to the diffraction limit of the light. Moreover, due to the weak linear and quadratic electro-optic effects in silicon, silicon-based optical modulators have large footprint [19], [22], [27]–[29]. These issues restrict the dense integration of optical modulators. This directed the research toward studying plasmonic materials and how to be combined with silicon-based EO modulators.

Since the discovery that light waves can propagate in the highly confined space at the interface between conductors and dielectrics, known as surface plasmon polariton (SPP), research in field of plasmonics has grown rapidly. Plasmonics offer curtailing the footprint of optical photonic modulators. Many Plasmonic materials have been investigated such as graphene, Silicon-germanium, vanadium dioxide, Gallium-doped zinc oxide, organics, III–V semiconductors and transparent conducting oxides (TCOs) [20], [30]–[37].

As shown in Figure 1.2, plasmonics are the solutions for the increasing demand of high operation speed and small size. They can work as a bridge between the speed of dielectric photonics and the size of silicon electronics [38]. The operation speed of silicon electronics is limited by the delay time of the electronic interconnects (to about 10 GHz); as well as, the size of the photonic devices is limited by the diffraction limit of light [39].

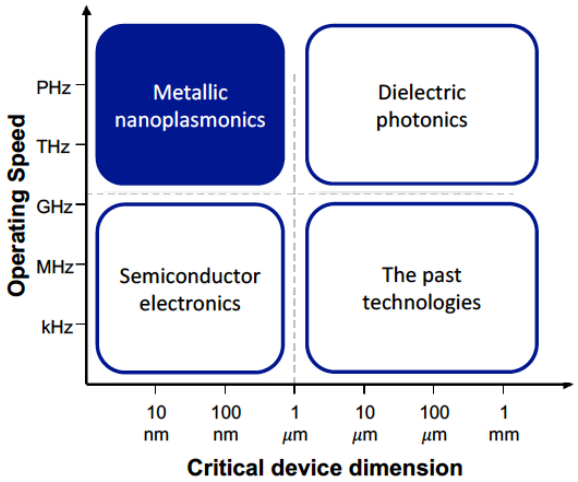

Figure 1.2 - Schematic summarizing the chip-device technologies for speed and size domains.

Adapted from [39].

Although, plasmonic electro-optic modulators can support very high modulation bandwidths, they have a high insertion losses because of the high field enhancement in the plasmonic metal based configurations [40]. This is a critical issue that raises the need for a low insertion loss optical modulators with high extinction ratio.

1.4 Thesis structure

In this chapter, the significance of electro-optical modulators for optical communication systems and for interconnects was emphasized. Also, the role of silicon photonics in revolutionizing the next generation of technology.

In the next Chapter 2 a brief background about the mechanisms, materials, and structures used for optical modulation is presented. In chapter 3, state-of-art EOMs are introduced.

In Chapter 4, an organic hybrid-plasmonic optical directional coupler is proposed and studied.

In Chapter 5, accurate description of epsilon-near-zero (ENZ) effect in indium-tin-oxide is discussed. Also, two hybrid silicon electro-optical modulators based on Indium-Tin-Oxide are proposed. The first is based on tri-coupled waveguides with electrical tuning mechanism that is designed to both the coupling conditions and introduces additional intrinsic losses. The second device is an electro-absorption modulator, based on dielectric slot waveguide with a plasmonic modulation section.

An optical switch based on a hybrid plasmonic-vanadium dioxide waveguide is presented in Chapter 6.

Last but not least, in Chapter 7, a brief summary and concluding notes are conveyed.

Chapter 2 Background

There are three fundamentals to describe optical modulators:

1. the modulation mechanism
2. the waveguide design
3. the martial

In this chapter, most of the mechanisms, designs, and materials related to optical materials will be reviewed. Furthermore, the key operating characteristics of optical modulators will be discussed.

2.1 External modulation mechanisms

Light can be modulated externally using different physical mechanisms, depending on the material used for modulation. Some transparent materials change their optical prosperities when subjected to an external perturbation, such as electric field, an acoustic wave, or increase in temperature. Acousto-optical effect and thermo-optical effect are discussed briefly since they are outside the thesis' focus.

2.1.1 Acousto-Optical effect

Some optical materials change their real and complex refractive indices when sound (acoustic) wave travels within, this phenomenon is known acousto-optical effect. Sound waves travel in the material crystal through the material's crystal compressions and rarefactions. Sound waves cause molecules to vibrate around their equilibrium, altering the polarisability and the refractive indices [12].

Acoustic wave takes time to travel across the light beam, limiting the switching speed and the modulation bandwidth [41]. Also, Si crystals does not utilize acousto-optical effect [12]. Consequently, CMOS optical modulators cannot be realized based on acousto-optical effect.

2.1.2 Thermo-optical effect

Thermo-optical effect is based on the fact that the refractive index of the material varies with the temperature. When the temperature increases, free carrier distribution changes, band-gap shrinks, and the crystal expands.

Studies shows that thermo-optical effect in Si is eight times higher than silica-based materials [42]. For Si, the refractive index variation as a function of temperature in in the range of 10^{-4} K^{-1} at 1.55 μm [43].

2.1.3 Electro-optical and electro-absorption effects

Some materials change their optical properties when subjected to external electric field. Appling electric field to such materials produces forces that alter the orientations, the shapes, and/or the positions of the molecules. The atomic response to the external electric field results in displacing atoms and electrons away from their equilibrium positions. Certain materials change their refractive index when an external electric field is applied. Other materials modify their absorption when an external electric field is applied; this is known as electro-absorption effect.

These two effects have been extensively studied as the foundation of the integrated optical modulators and the optical communication systems [44]. Both electro-optical effects and electro-absorption effect are very fast with sub-picosecond time response [6]. The speed of modulators based on these effects are restricted by technological limitations, rather than the basic effects themselves [6].

2.1.3.1 Electro-optical effects

Electro-optical effect is based on change of the optical properties upon on applying external electric field to the material; it controls the intensity, phase and/or polarization. Electro-optical effect can be either linear or quadratic [12]. The linear electro-optic effect is known as Pockels effect; the quadratic electro-optic effect is known as Kerr effect.

Since the refractive index n changes slightly with the applied electric field, it can be expanded with Taylor's series as in (2-1):

$$n(E) \simeq n - \frac{1}{2} r n^3 E - \frac{1}{2} \xi n^3 E^2 \qquad (2\text{-}1)$$

where r is the Pockels coefficient and ξ is the Kerr coefficient [12].

2.1.3.1.1 Pockels effect

Pockels effect is found in materials with crystals that does not have inversion symmetry (centro-symmetric structure) and electro-optical polymers [6]. When the second term in Equation 1 is many orders of magnitude higher than the third term, the medium is considered as Pockels medium.

Pockels effect is sensitive to the direction of the applied electric field as well as the polarization of the propagating light [6]. The most commonly used electro-optical materials based on Pockels effect are lithium niobate ($LiNbO_3$) and III-V semiconductors. Si does not have such effect due to its centro-symmetric crystal structure [12].

2.1.3.1.2 Kerr effect

In centro-symmetric crystal materials, the second term in Equation 1 vanishes and the refractive index depends on the third term [12]. Kerr effect is common in all transparent nonmetallic materials. The applied electric field breaks the symmetry of the crystal and, sequentially, allows for change in the refractive index [6].

The kerr effect in Si carefully studied and modeled by Soref and Bennet [19]. They studied the change in the refractive index in a crystalline silicon at room temperature. The study shoes that the change in the refractive index is in the range of 10^{-4} at an electric field around 10^6 V/cm; this value of electric field is beyond the breakdown value in lightly doped Si.

2.1.3.2 electro-absorption effect

Electro-absorption effect, also based on applying external electric field to the material[2], is when the change in the refractive index is due to Kramers-Kronig transformation of the absorption band edge. In bulk semiconductors it is known as Franz–Keldysh effect [44].

An applied electric field causes a distortion of the energy bands (conduction and valence) in semiconductors, thus the photo-absorption coefficient (α) rises when the band edge energy threshold shifts towards lower energies. Photons can tunnel across the bandgap with energies lower than band-to-band. This results in both phase and intensity modulation [6].

When in direct band gap semiconductors, α increases steeply, while in indirect bandgap semiconductors, such as Si, α has a smaller increase [12].

[2] Both electro-optical and electro-absorption effects are based on applying external electric field to the material. A small terminology note: most of the time electro-optical effect refers to the linear Pockels effect and the quadratic Kerr effect [44]. In other contexts, the the linear Pockels effect, the quadratic Kerr effect, electro-absorption effect, and carrier density effects are referred to as electro-optic effects [6].

2.1.4 Carrier density effects

Carrier density in semiconductors is related to several effects: bandgap shrinkage, band filling, and free-carrier absorption (plasma dispersion effect) [6]. The optical properties can be changed by injecting free carriers to the un-doped material or by removing free carriers from the doped materials. This mechanism exploits changes in the density of the free carriers in the semiconductor material to modulate the real and imaginary parts of the refractive index [35]. Photons are absorbed by the free carriers causing intra-band transitions.

Electrical inducing of the carriers can be through either injecting in PIN diodes or the field effect formation, carrier-depletion and accumulation, in metal-oxide-semiconductors (MOS) and reverse-biased PIN junctions. This imposes major speed limitations due to the lifetime of the carriers.

Due to the strong coulombic effects in the crystalline Si, free carrier concentration effect is the most important modulation mechanism affecting the real and imaginary parts of the refractive index of Si [12]. However, the speed is limited due to the lifetime of the carriers which is in the range of 1 ns–10 ns for pure Si [6]. Free carrier concentration effect can be theoretically described using the Drude model [45], [46].

2.2 Different optical modulators structures

Linear and quadratic electro-optic effects change the phase of the optical wave; detecting such a phase change is very complicated since it requires coherent optical receiver. Hence, several modulation designs developed to modulate the intensity of the light using the phase change produced from electro-optic effects.

2.2.1 Electro-absorption Modulator (EAM)

EAMs are based on Electro-absorption materials to modulate the intensity of the light directly. The design is very simple: it is one waveguide (WG) with two electrodes for applying the electric field to modulate the intensity.

III-V material are the best materials used to build EAMs. Such modulators are very compact, with high extinction ratios, and need low drive voltages [6]. Figure 2.1 shows the general schematic and transfer function of EAM.

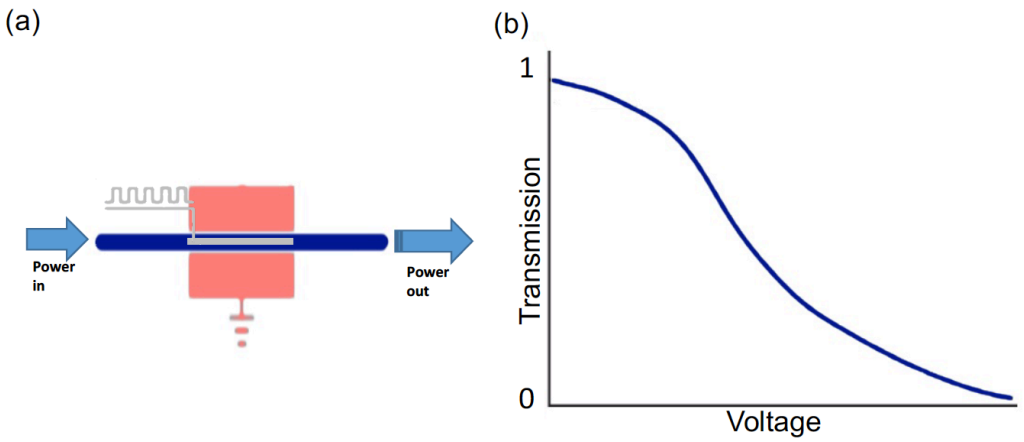

Figure 2.1 - General electro-absorption modulator (a) schematic and (b) transfer function.

Adapted from [6].

2.2.2 Mach-Zehnder (MZ) modulator

MZ interferometers are very successful modulators since they use the phase change to modulate the intensity directly. Light enters the modulator from one WG, then the light splits into two WGs (arms) of the interferometer. Linear and/or quadratic EO effects are used to modulate the phase of the light traveling in one of the arms to be completely out of phase with respect to the other arm. At the output, the two arms merge recombining the light again.

In 1x1 designs, depending on the modulation state, light recombines either constructively or destructively. Thus, the intensity of the light is modulated. In the off-state, light in the two arms are in phase, light is transferred to the output port [3]. In the on-state, light in the two arms are out of phase, light is radiated. In 1x2 designs, the light gets out either from the first arm of from the other depending on the modulation state.

Figure 2.2 shows the general schematic and transfer function of MZ interferometer modulator.

[3] Throughout the whole thesis, off-state and on-state are referring to the states with external modulating voltage is off and on, respectively, not the optical power.

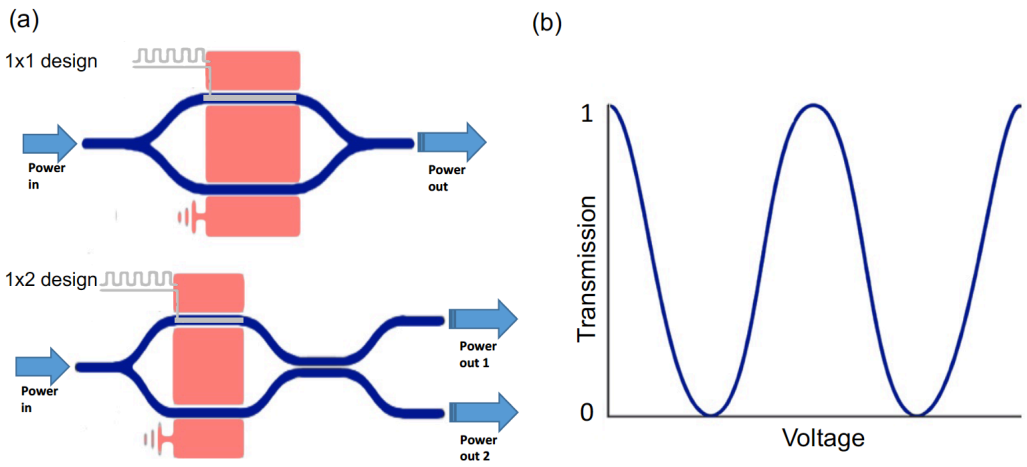

Figure 2.2 - General Mach-Zehnder interferometer modulator (a) schematic and (b) transfer function.

Adapted from [6].

2.2.3 Resonant modulator

Resonant modulators are based on the operation principle of optical filters; they work on band-pass filters. The input optical frequency is very close to the filter's band-pass frequency. When the modulation is turned on, the filters frequency shifts, changing the transmission properties.

The resonant modulator, such as ring resonator modulator, the input, multiple wavelength, power couples from the input/output WG to the ring. If, for example, certain wavelength λ_i satisfies (2-2), λ_i will be suppressed in the ring, while the rest of the wavelengths will couple back to the output WG.

$$\lambda_i = \frac{n_{eff}\ L}{m} \tag{2-2}$$

When the modulation voltage is applied to the electrodes, the effective refractive index of the ring changes, the optical path length changes varying the resonant frequency. Figure 2.3 shows the general schematic and transfer function of ring resonator modulator.

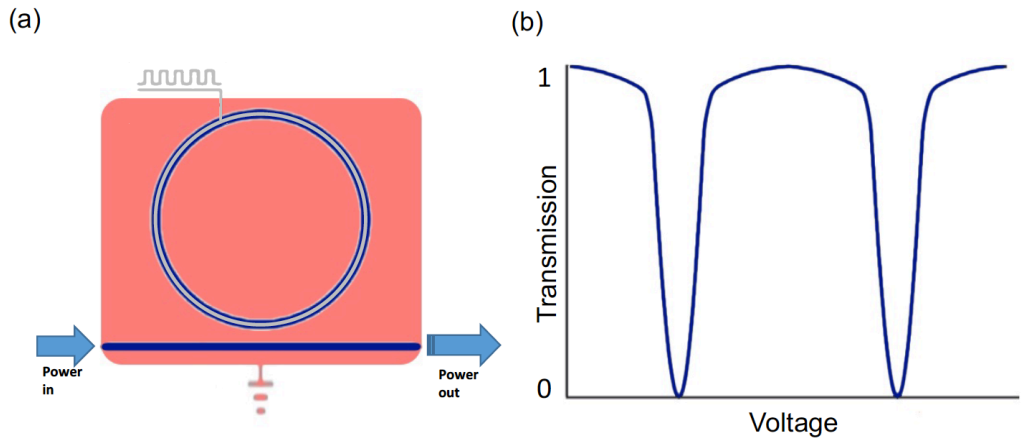

Figure 2.3 - General ring resonator modulator (a) schematic and (b) transfer function.

Adapted from [6].

Not only rings can be implemented for resonant modulators, but also different other designs can be implemented such as discs and Fabry-Perot resonators [6].

2.2.4 Directional coupler (DC) modulator

Another design worth mentioning for modulators is the Directional couplers. Directional couplers' structures involve two identical adjacent WGs that come close to each other, creating a coupling environment [47]. This results in two modes; a symmetric (even) mode, with an effective refractive index greater than that of a single waveguide, and an anti-symmetric (odd) mode, with an effective refractive index smaller than that of a single waveguide.

The interaction between these modes results in the power being fully coupled to the other channel after a specific distance, the beating length, (L_B) defined as:

$$L_B = \frac{\lambda}{2(n_{even} - n_{odd})} \qquad (2\text{-}3)$$

Where λ is the wavelength of the optical wave, and n_{even} and n_{odd} are the effective refractive indices of the fundamental symmetric mode and anti-symmetric mode respectively.

The amount of the power couples from one arm to the other can be controlled by applying voltage to one of the arms. In other words, applying voltage to the electrodes changes the effective refractive indices of the fundamental symmetric and anti-symmetric modes resulting in changing the L_B. thus, the amount of the power couples from the first WG to the other changes. Figure 2.4 shows the general schematic and transfer function of DC modulator.

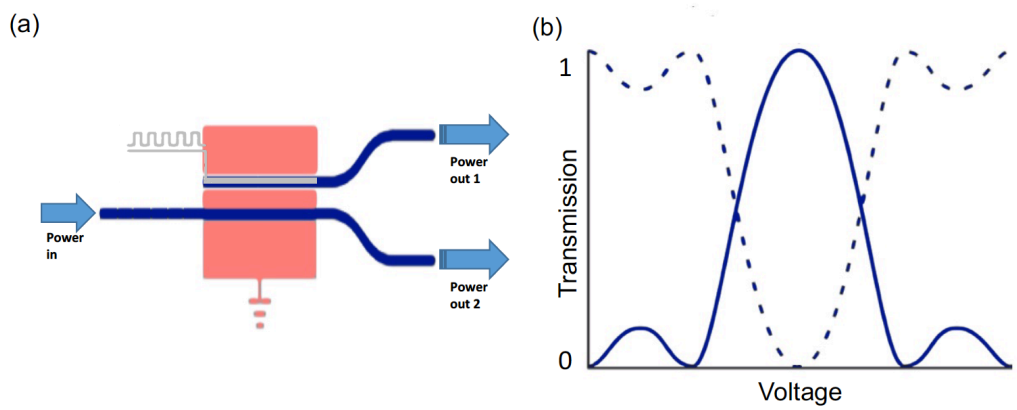

Figure 2.4 - General directional coupler modulator (a) schematic and (b) transfer function.

2.3 Materials

The most important aspect in designing any modulator is the material. The modulator material determines most of its characteristics and properties. It determines the electro-optic effects possible, the complexity of its fabrication, and its reliability. Modulator materials should have some basic requirements such as transparency at the operating wavelength and strong electro-optic effect. There are also some technological requirements such as the fabrication methods, and the stability over operating temperature range [6]. In this section, the major classes of materials used for modulators will be reviewed.

2.3.1 Inorganic crystals

From the prospective of modulators inorganic crystals are either lithium niobate ($LiNbO_3$) or everything else.

2.3.1.1 Lithium niobate ($LiNbO_3$)

$LiNbO_3$ is very common for conventional commercial modulators. It is very developed and many designs are based on it [48]. It satisfies all the fundamental requirements mentioned before; it is transparent over a wide range of frequencies, has strong Pockels effect, and can be easily fabricated [6]. More importantly, $LiNbO_3$ is not compatible with the wide spread CMOS technology.

$LiNbO_3$, also, has some problems. It is a ferroelectric material; it has an electric dipole built-in that strongly depends on the temperature [49].

2.3.1.2 Other inorganic crystals

There are others inorganic crystals that studied and used for optical modulation such as potassium titanyl phosphate (KTP) and lithium tantalite ($LiTaO_3$). Their EO coefficients are very similar to LiNbO3 and have better power handling prosperities [6].

There are other inorganic crystals with even higher EO coefficients. For example, barium titanate has EO coefficient that is 58 times the EO coefficient of LiNbO3 [6]. It is very useful for low voltage modulators [50]. However, it has many drawbacks; its dielectric constant fluctuates with frequency and it is very temperature dependent especially over room temperatures.

2.3.1.2.1 Vanadium dioxide (VO_2)

A worth mentioning inorganic crystal, that is believed to revolutionize the photonic industry, is vanadium dioxide. It is considered as a phase change material. It undergoes a transformation from semiconductor state to metallic state when subjected to external stimulus, such as change in temperature and potential difference [51]. It has been integrated with photonic structures to achieve optical modulation [52].

The change in the complex refractive index of VO_2 is in the range of unity. Modulators based on VO_2 as the plasmonic material have shorter device length compared with other active materials. Yet, VO_2 has high material absorption in the semiconductor state, which leads to high propagation losses [51].

2.3.2 Semiconductors

Semiconductors are very attractive for both the photonics and electronics industries. Semiconductors offer, more EO effects, compared to insulators, such as electro-absorption and carrier density effects. They offer integration not only with electronic circuitries, but also with lasers.

2.3.2.1 III-V Semiconductors

So far, these materials are the most important materials in the photonic world; most lasers, detectors, transistors and modulators are made in these materials. The III-V semiconductors are the compounds of the third and fifth group elements in the periodic table, such as gallium arsenide and indium phosphide. They are available in wafers. The most common optical modulators built in these materials are EAMs. In III-V

semiconductors, the quadratic EO effect is better than the linear EO effect, but it is associated with absorption [6].

2.3.2.2 silicon

Silicon is the base for electronic industry. Thus, it is very appealing for integrated optics. However, its EA effects are very weak. As discussed in the previous section, the linear EO effect is not present, the quadratic EO and EA effects are very weak. Carrier density effect is used to achieve modulation in Silicon.

Silicon is not the best material for designing optical modulators. The research has moved toward hybrid designs, where silicon is combined with other materials with strong EO effects. Hybrid designs have many advantages such as the low optical losses of silicon, the integration with electronic circuits, and the strong EO effects of the active materials.

2.3.3 Polymers

Polymers are organic insulating materials, that uses linear Pockels effect to modulate light. Usually, they are prepared in liquid form, then spun over the substrate and then cured to form thin films. WGs based on polymers have very low propagation loss at the telecommunication wavelength.

Polymers have many advantages, such as they can be spun on films over any substrate forming active layer. They have high EO coefficients as high as five times higher than LiNbO3 [53]. There is one main drawback to polymers which is thermal instability [54]. Chemical engineers study new forms of polymers to optimize the tradeoff between the EO coefficient and thermal instability [6]. Also, polymers suffer from weak optical power handling [55].

2.3.4 Transparent conducting oxides (TCOs)

TCOs are very promising because they are CMOS compatible. Indium-tin-oxide (ITO) is the most widely used TCO. Using ITO as the plasmonic material for EOM attracted a lot of research due to its wide bandwidth [34]. Yet, it suffers from high insertion losses due to the strong field enhancement in the lossy plasmonic waveguides.

Carrier density of ITO can be utilized when used in MOS-structures [56]. ITO exhibits high electrical conductivity and has plasma frequency upon applying electrical

(gate) voltage, which results in epsilon-near-zero (ENZ) effect [57], [58]. In other words, formation of this accumulation layer can tune plasma frequency and permittivity significantly. ITO modeling is discussed in details in Chapter 5.

2.4 Key operating characteristics of optical modulators

In this section common optical modulators characteristics and performance measurements are discussed. These factors are very important for designing and evaluating EOM.

2.4.1 Extinction ratio (ER)

Extinction ratio is defined as the output optical power when the modulator is operating at the "off-state" to the output optical power when the modulator is operating at the "on-state." It should be measured at low-frequency operation or DC [6]. ER, always stated in decibels, is given by:

$$ER_{dB} = 10\ \log\frac{P_{off}}{P_{on}} \tag{2-4}$$

where P_{off} and P_{on} are the output optical power at the odd-state and on-state, respectively [59].

ER is very important because low ER causes power penalty in digital communication systems [6]. Higher ER is always required for optical modulators.

2.4.2 Insertion loss (IL)

Insertion loss is another important parameter for EOM. It is defined as the input optical power to the output optical power when the modulator is operating at the "on-state." IL is defined in decibels as:

$$IL_{dB} = 10\ \log\frac{P_{in}}{P_{out}} \tag{2-5}$$

where P_{in} and P_{out} are the input optical power and the input optical power at the off-state, respectively [60].

IL is very important for the power efficiency factor. The performance of the modulator is determined output optical power. The higher the IL, the more powerful the light source is required to achieve high performance.

2.4.3 Energy consumption and modulation speed limit

Energy consumption is a very important parameter for EOMs because it determines its modulation speed limit. Energy consumption is related to the Capacitance and the modulation voltage of the modulator. The energy consumption per bit can be estimated using:

$$E/_{bit} = \frac{CV^2}{2} \tag{2-6}$$

where C is the capacitance of the modulator and V is the modulation voltage.

The modulation speed limit is defined as:

$$f_{max} = \frac{1}{2\pi \cdot RC} \tag{2-7}$$

where R is the resistance of the device including the interconnects and C is the capacitance of the modulator.

Chapter 3 Recent advances in electro-optical modulators

Many research groups have reported electro-optic modulators with speeds exceeding 10 GHz. In this chapter, some of these state-of-the-art electro-optic modulators will be reviewed. The modulators reviewed are based on different structures and across several active materials[4]. As discussed earlier, pure silicon linear electro-optic effect is not found; quadratic electro-optic effect is weak at the telecommunication wavelength, so silicon-based optical modulators have large footprint [19], [22], [27]–[29]. Plasma dispersion effect is the most common modulation mechanism in Silicon [12]. However, the speed of these devices is limited. 1 GHz –10 GHz, due to the lifetime of the carriers [6]. This raised the necessity for investigating other novel alternative active materials [20], [30]–[37]. Organic polymers, Indium-tin-oxide (ITO), and vanadium dioxide are among the materials investigated for modulation applications [61], [62].

3.1 Silicon based electro-optical modulators

Plasmonic designs that uses Si as the active material are proposed. “PlasMOStor” is based on modulating plasmonic waves in Ag/SiO_2/Si/Ag MOS vertical configuration [63]. The schematic for this design is shown in Figure 3.1(a). This design is not easy to integrate to standard Si chips [64]. This plasmonic modulator can achieve extinction ratio approaching 10 dB with a potential for gigahertz modulation bandwidth. This design is not easy to integrate to standard Si chips [64].

Zhu *et al.* fabricated a CMOS nano-plasmonic modulator based on a horizontal metal-insulator-silicon-insulator-metal slot waveguide [64]. The modulation mechanism is based on electricaly inducing free charge accumulation layer at the Si/insulator interface. The design is 4 μm long and offers a 3 dB/μm extinction ratio per unit length. Its speed is less than 1 GHz and is not easy to fabricate. The schematic for this design is shown in Figure 3.1(b).

[4] The designs chosen based on the relevancy to the thesis work.

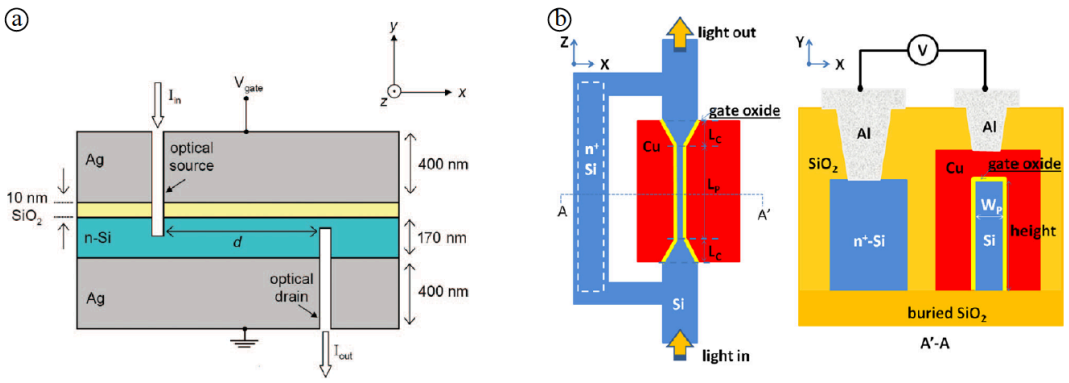

Figure 3.1 - Plasmon EOMs that uses Si as the active material. (a) Cross-sectional schematic of the Ag/SiO2/Si/Ag MOS vertical configuration (plasmostor). (b) top view and cross-sectional of the metal-insulator-silicon-insulator-metal Si nano-plasmonic electro-absorption modulator.

Adapted from American Institute of Physics and American Chemical Society with permissions [63] and [64].

In order to overcome these speed limitations, different active materials have been studied, such as organic polymers, inorganic crystals, and transparent conducting oxides (TCOs) and [20], [30]–[37]. Hybrid Modulator designs offers high operation speeds compared to designs that use Si as active materials.

3.2 EOP based electro-optical modulators

Among organic polymers, Kim *et al*, engineered an electro-optical polymer (EOP) based on self-organized molecular glasses that is thermally stable [53]. This polymer has an excellent optical transparency and an electro-optic coefficient of r_{33} = 300 pV/m, that is five times higher than LiNbO3. Many electro-optical modulators are based on this EOP [65], [65]–[68].

Among these designs, Sun *et al.* proposed an modulator based on silicon-polymer-metal hybrid plasmonic waveguide [66]. The device length is 13 μm. The device has an insertion loss of 7.7 dB and an extinction ratio of 12 dB. The speed of the device is only 90 GHz. The schematic is shown in Figure 3.2 (a). Its modulation properties are summarized in Table 3-1.

Another design based on this EOP was proposed by Janjan *et al.* [65]. It is a ring resonator modulator based on polymer filled hybrid plasmonic waveguide. The device has a footprint of 11.2 μm_2; ~ 2.3 dB insertion loss and ~ 8 dB extinction ratio are achievable at the telecommunication wavelength. The schematic of this device is shown in Figure 3.2(a); as well as, its modulation properties are summarized in Table 3-1.

Also, Zografopoulos realized a directional coupler based modulator using this EOP. An extinction ratio of 22.2 dB is achieved at 52.7 μm device length. The modulation properties are summarized in Table 3-1.

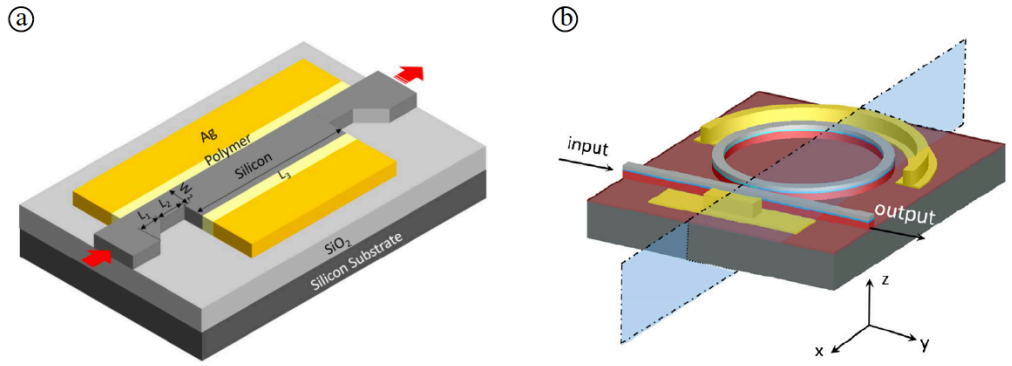

Figure 3.2 - EOP based plasmonic modulators. (a) schematic view of silicon-polymer-metal hybrid plasmonic EO modulator. (b) Schematic of the ring resonator modulator based on polymer-filled hybrid plasmonic waveguide.

Adapted from Institute of Electrical and Electronics Engineers and Springer International Publishing AG. with permissions [66] and [65].

3.3 ITO based electro-optic modulators

Another optical active material that is used, recently, for modulation is ITO; many devices are realized [40], [69]–[73]. Among these designs, Zhao *et al.* proposed an EA modulator based on a hybrid Si slot waveguide [74]. This device is based on 2D electromagnetic simulations. The length of the device is estimated to be from 1.25 to 1.42 μm and achieving 6 dB and 1.3 dB for insertion loss and an extinction ratio, respectively. The modulation properties are summarized in Table 3-1.

Lee *et al.* fabricated and tested “PlasMOStor” modulator [75]. The device is based on an Au plasmonic slot waveguide filled with ITO. The schematic of this modulator is shown in Figure 3.3 (a). The modulation properties are provided in Table 3-1. The measurements demonstrate that a 0.45 dB insertion loss and ~ 2.71 dB extinction are realized for a 10.28 μm device length.

Another group, realized an EO modulator based on an ITO-integrated directional coupler [73]. The schematic of this modulator is shown in Figure 3.3 (b). This device achieves ~1 dB insertion loss and ~6 dB extinction for a 5.6 μm device length. The rest of modulation properties are provided in Table 3-1.

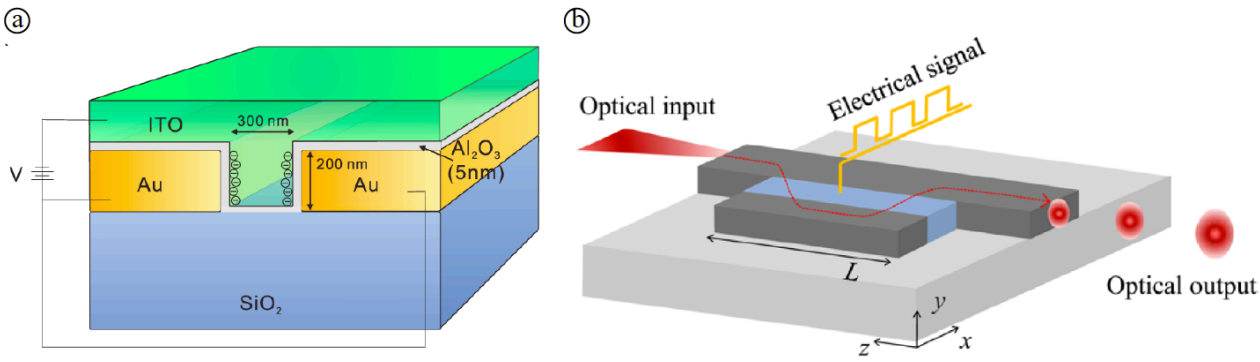

Figure 3.3 - ITO based plasmonic modulators. (a) Cross-sectional schematic view of the "plasmostor" based on Au plasmonic slot waveguide filled with ITO. (b) Bird's eye view of the silicon electro-optic modulator based on an ITO-integrated tunable directional coupler.

Adapted from IOP Publishing and American Chemical Society with permissions [73] and [75].

3.4 VO_2 based electro-optic modulators

The last plasmonic active material to be considered throughout the thesis is vanadium dioxide. As discussed in the previous chapter, it is believed to revolutionize the photonic industry due to its transformation from dielectric state to metallic state. Many EOMs based on this phase change property were realized [51], [52], [76]–[79].

Markov *et al.* presented an EO modulator based on near-field plasmonic coupling in Au hybrid plasmonic waveguide [80]. The coupling is between a thin film of vanadium dioxide on a silicon substrate and gold nanodisks. The schematic of this device is shown in Figure 3.4 (a). The modulation properties are summarized in Table 3-1.

Another design which is based on Ag hybrid plasmonic waveguide was fabricated [81]. The results are very promising in terms of bandwidth. Also, 20 dB modulation depth is achieved at a very low voltage of 400mV. The rest of modulation properties are provided in Table 3-1.

Wong *et al.* studied and proposed an EOM based on hybrid plasmonic surface plasmon polariton (HPSPP) waveguide with a VO_2 layer on the top [82]. What is interesting about this design is that the mode is confined in the silicon layer to minimize the insertion losses resulting of the mode confinement in the VO_2 layer. The schematic of modulation section of this device is shown in Figure 3.4 (b). The device is compact with a 2 μm modulation length. The modulator achieves ~2.8 dB insertion loss and ~7.6 dB extinction ratio. The modulation properties are summarized in Table 3-1.

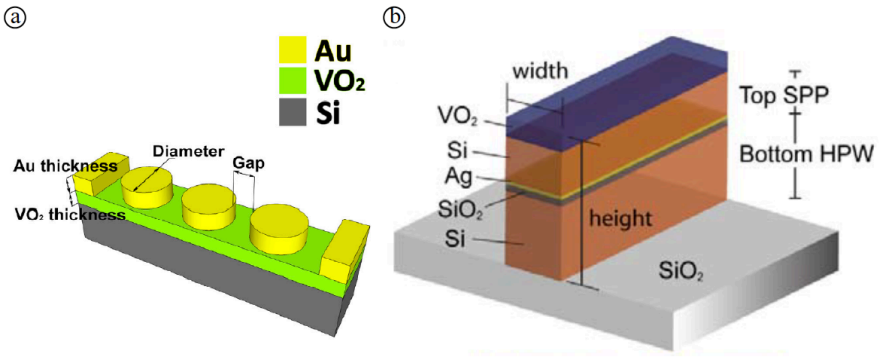

Figure 3.4 - VO2 based plasmonic modulators. (a) Schematic view of Au nanodisks hybrid plasmonic waveguide. (b) Schematic of the modulation section of the electro-optic modulator based on HPSPP/VO2 waveguide.

Adapted from OSA Publishing and American Chemical Society with permissions [73] and [75].

Table 3-1 – Comparison of the modulation properties for different EOMs utilizing different active materials that have been reported and related to the scoop of the thesis.

Device type	Active material	Experimental/ theoretical	Operation wavelength [μm]	ER [dB]	IL [dB]	Device length/ footprint	Modulation Voltage [V]	Energy/ bit [fJ]	Speed
Cu hybrid plasmonic waveguide [64]	Si	Experiment	1.55	1.9	1	3 μm	<~4	**	<1
silicon-polymer-metal hybrid plasmonic waveguide [66]	EOP	Theoretical (FEM)	1.55	12	7.7	13 μm	6	24.4	90 GHz
Polymer-Filled Hybrid Plasmonic ring waveguide [65]	EOP	Theoretical	1.55	~8	~2.3	11.2 μm^2	6	3.6	1 THz
directional couplers enhanced with a layer of electro-optic polymer [83]	EOP	Theoretical (FEM)	1.55	22.2	2.8	52.7 μm	3.1	62	Tens of GHz
ITO based on a hybrid Si slot waveguide [74]	ITO	Theoretical (2D)	1.55	~6	~1.3	1.25 to 1.42 μm	~2–4	**	**
Au plasmonic slot waveguide [75]	ITO	Experimental	1.55	2.71	0.45	10.28 μm	~1.2	4	<100 GHz
ITO-integrated directional coupler [73]	ITO	Theoretical (FEM)	1.55	~6	~1	5.6 μm	2.3	330	25.68 GHz
Plasmonic nanodisk chain Si-Au-VO_2 [80]	VO_2	Theoretical (3D FDTD)	1.55	8.9	12.5	0.56 μm	0.4	**	~1 GHz
Ag hybrid plasmonic waveguide [81]	VO_2	Experimental	1.55	16.1	6	7 μm	400×10^{-3}	**	400×10^{-9} GHz
Si wire/VO2 waveguide [82]	VO_2	Theoretical (3D FDTD)	1.55	7.6	2.8	2 μm	**	250	~1 GHz

Chapter 4 Organic based electro-optical modulators

Design 1: Hybrid silicon plasmonic organic directional coupler based modulator [5]

Abstract

In this chapter an organic electro-optical modulator based on hybrid-plasmonic directional coupler is proposed. The directional coupler is based on silicon-polymer-metal hybrid plasmonic waveguides. The power power-splitting mechanism utilizes the electro-optical properties of the embedded polymer layer to tune the power upon applying external electric field. The directional coupler based modulator operates under the telecommunication wavelength (1550 nm). A finite element method with a perfect matching layer (PML), are taken up to simulate and analyze the electro-optical modulator.

4.1.1 Introduction

The growing demand for high capacity systems resulted in replacing electronic baseband systems with optical broadband systems. Optical communication systems are superior to electronic communication systems in many aspects such as high bandwidth, low cost, and low transmission losses for long distances. In an optical communication system, switching and modulation are principle operations [6].

Electro-optical modulators (EOMs) attracted a lot of research interest. Many aspects should be considered while designing an EOM such as high bandwidth, high extinction ratio, low insertion loss and CMOS-compatibility.

During the same time that demand for optical communication systems increased, noteworthy development has happened in the field of silicon photonics. The material system used for electronic circuitries for many decades, now is used to build optical integrated devices and circuits. Silicon photonics is very appealing since it uses the existing CMOS-VLSI technology, and cheaper for mass production. Also, silicon is almost transparent at the telecommunication wavelengths.

Many configurations and designs for Si-based optical modulators have been developed, including, but not limited to, Mach–Zehnder interferometer (MZI), ring

[5] Parts of this section were previously published in [A] and [B].

resonator, metal-oxide- semiconductor capacitor, and micro-disk structure [20]–[23], [28], [84]–[86]. MZIs are not effective due to its large sizes; as well as, disk and ring resonators are not effective due to their narrow bandwidth [19]. For a compact modulator with a high bandwidth, modulators, based on plasmonic electro-optic waveguides, have been studied [24], [30], [61], [63], [70], [87], [88]. Among plasmonic electro-optic modulators, directional coupler based modulators show promising results both in terms of size and bandwidth [40], [68], [89].

Pure silicon linear electro-optic effect is not found; quadratic electro-optic effect is weak at the telecommunication wavelength, so silicon-based optical modulators have large footprints [19], [22], [27]–[29]. Plasma dispersion effect is the most common modulation mechanism affecting thr refractive index of silicon [12]. However, the speed of these devices is limited, 1 GHz –10 GHz, due to the lifetime of the carriers [6]. This raised the necessity for investigating other novel alternative active materials [20], [30]–[37].

$LiNbO_3$ is very common for conventional commercial modulators. It is very developed and many designs are based on it [48]. It satisfies all the fundamental requirements mentioned before; it is transparent over a wide range of frequencies, has strong Pockels effect, and can be easily fabricated [6]. However, $LiNbO_3$ is not compatible with the wide spread CMOS technology. $LiNbO_3$ is, also, temperature sensitive [49].

Introducing polymers to optical modulation, the fundamental requirements can be achieved without compromising the CMOS compatibility.

Polymers offer very high Pockels coefficients up to 300 pV/m [90], [91] and a purely electronic hyperpolarisability [92]. These advantages can offer modulation speeds up to 150 GHz depending on the capacitance of the device. Polymers also offer moderate refractive indices around $n \approx 1.6$. Brosi et al. proposed the concept to combine both silicon and polymers to attain high speed modulation [93].

Polymers have low dispersion profile in the range of telecommunication wavelength and large electro-optic coefficient. Switching time and frequency depend on many factors, such as response time of the electro-optic polymer materials [68]. Since the response time of almost all polymers as fast as femtosecond, we can consider that there is no delay between the change of the electric signal and that of the refractive

index of the electro-optic polymer [94]. Then, the effective refractive index of the plasmonic mode can be modulated effectively.

Although, plasmonic electro-optic modulators can support very high modulation bandwidths, they have a high insertion losses because of the high field enhancement in the plasmonic metal based configurations [40]. This is a critical issue which raises the need for a low insertion loss plasmonic optical modulator with high extinction ratio.

To satisfy this need, in this work we introduce an electro-optic plasmonic modulator. The modulator is based on a directional coupler which supports a symmetric and an anti-symmetric modes when no external voltage is applied. The power splitting mechanism of the modulator is based on changing the refractive index of the EOP by applying external electric field such as that one mode is allowed to propagate. A finite element method with a perfect matching layer (PML) absorbing boundary condition is used to simulate and calculate the insertion losses, propagation losses and the power splitting ratios between the two channels. We have succeeded in designing a hybrid silicon plasmonic organic directional coupler based modulator with 14.34 dB extinction ratio of the power on the on-state to the off-state at the length of the modulator, 39 μm. We estimated the insertion losses to be 2.298 dB.

In the next section, the design will be introduced; then, the principle of operation will be discussed. In the third section, results are presented. Finally, in the fourth section a brief summary and concluding notes are conveyed.

4.1.2 Design

The proposed directional coupler is based on creating two high index EOP waveguides surrounded with low index regions as shown in Figure 4.1.

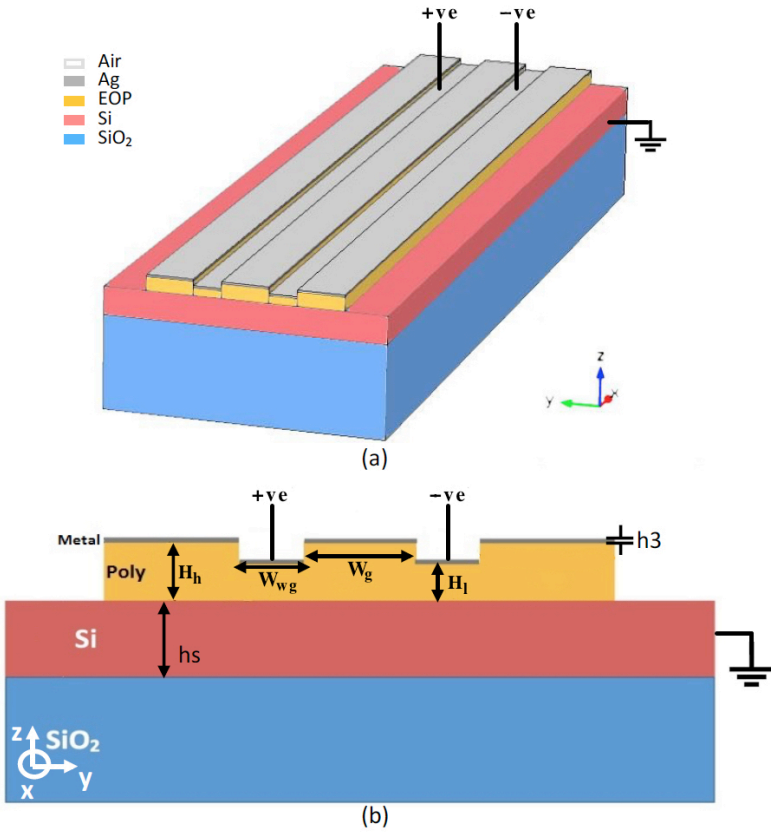

Figure 4.1 - (a) Schematic layout (Bird's eye view) and (b) cross-sectional of the proposed electro-optic plasmonic directional coupler modulator.

The device can be fabricated on silicon-on-insulator standard wafer. A thin layer of an electro-optic polymer (EOP) is spin-coated on the top of silicon; EOP is etched over two regions defining the low height (high index) regions. Finally, a silver layer is deposited on the top of EOP regions to define the guiding regions.

4.1.2.1 Principle of operation

The optical wave is confined in the EOP layer of the high index (low height) regions. One mode is excited through the first waveguide. When there is no external electric field is applied, the power couples back and forth from one waveguide to the other.

The modulation technique is based on applying a positive electric field to one of the waveguides and a negative electric field to the other waveguide while keeping the Si layer grounded. Applying electric fields in such a way changes the refractive index of

the EOP in these two waveguides due to the Pockels effect [95]. This results in changing the effective refractive indices of the symmetric and anti-symmetric propagating modes.

Drude model is used to describe the change in the refractive index of the EOP. The refractive index of the EOP is n_{poly} = 1.65 and its electro-optic coefficient r_{33} = 300 pV/ m [91]. The polymer has an excellent optical transparency (has negligible lose) at the telecommunication wavelength range [96]. Also, Sellmeier model used to describe the dispersion of Si and SiO2 [97].

When applying electric field to the EOP layer, the refractive index changes as in:

$$\Delta n_{poly} = \frac{1}{2} {n_{poly}}^2 r_{33} E_{RF} \quad (4\text{-}1)$$

Modal analysis used to optimize the dimensions. To realize a compact coupler design, the beating length L_B is reduced by decreasing the gap width. The optimized gap width is 500 nm because further reduction results less confinement of the mode in the low height regions and the more confinement in the gap between the two low height regions; Thus, the effect of applying external electric field will become of less effective. The dimensions that have great effects on the effective refractive index are h_h and h_l. The dimension h_l is set as small as possible to reduce the voltage needed to generate change in the refractive index of the EOP.

The design goal is to match the effective refractive index of the low region (h_l) for the negatively biased state to that of the high regions (h_h). The height h_h is set to be 125 nm to be large enough to raise the difference between h_h and h_l for two reasons. Firstly, to avoid contact of the metal layers of the high regions with low regions; secondly, to avoid electric field confinement between the metal edges. For w_g = 500 nm, w_{wg}= 300 nm, and h_h= 125 nm, the effective refractive index of the high region (h_h) is 1.656 and the effective refractive index of the low region (h_l) when a negative voltage is applied changes from 1.65 to 1.664. Figure 4.2 shows the dependence of the effective refractive index on h_l for the biased low region versus the effective index of h_h equals 125 nm for the unbiased low region. It is evident from the graph that the point of operation is where the effective indices are equal; at which h_l= 60 nm. Figure 4.3 shows the effective refractive indices for each regions for both the off and on states.

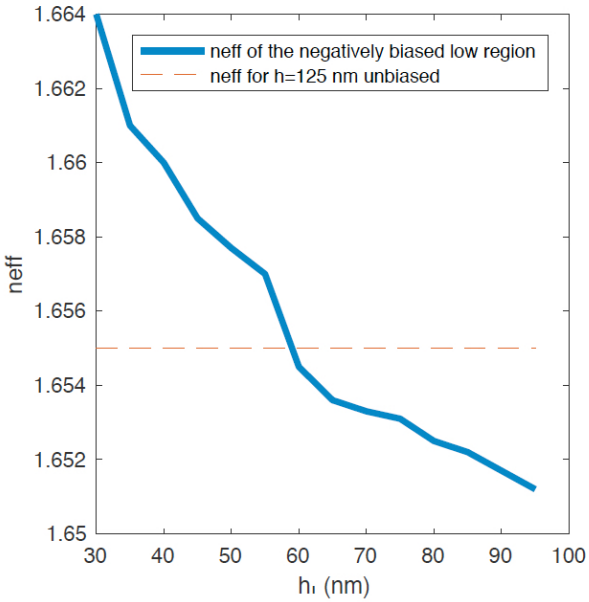

Figure 4.2 - Dependence of the effective index on hl for the negatively biased low region vs the effective index of h_h equals 125 nm for the unbiased low region.

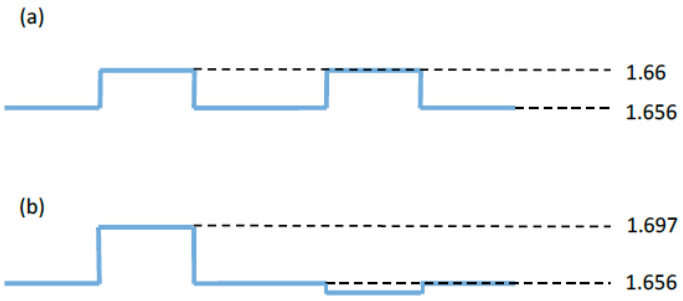

Figure 4.3 - the effective refractive index of each region for (a) the off and (b) on states.

4.1.2.2 Single channel waveguide

The electric filed mode profile of a single waveguide is shown in Figure 4.4. The optical power is confined in the low height (h_l) polymer region.

Mode analysis shows that the real part of the effective index of the mode in Figure 4.4 is 2.703 for the off-state and 2.732 for the on-state; and the propagation losses are calculated, to be 0.0587 dB/μm and 0.0722 dB/μm for the off-state and the on-state respectively.

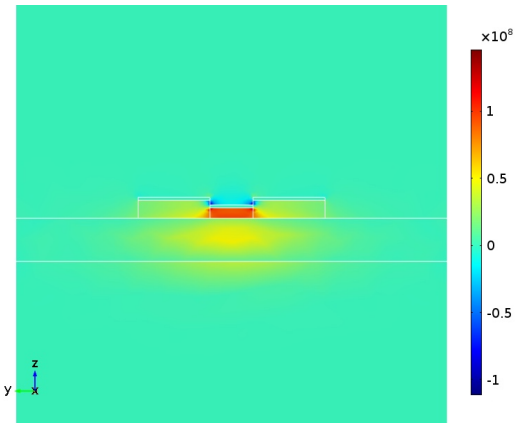

Figure 4.4 - The field distribution (|Ez|) of the single channel mode at the off-state.

4.1.2.3 Two channel waveguide

4.1.2.3.1 Off-state

When there is no external electric field is applied to the two waveguides (off-state), the refractive index of the polymer is the same everywhere. The input mode is excited through one of the waveguides. This mode resolve into two, even and odd, modes. Figure 4.5 shows the electric filed mode profile of those two modes, namely, the even (symmetric) mode with an effective index equals 2.7612, and the odd (anti-symmetric) mode with an effective index equals 2.703.

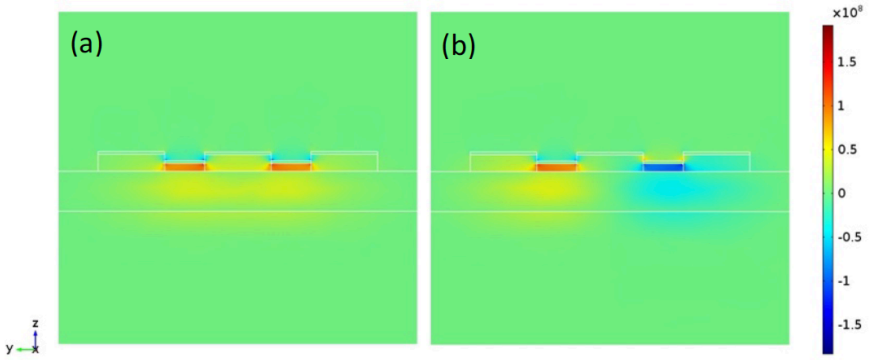

Figure 4.5 - The z-component of the field for (a) the even mode in the off state, (b) the odd mode in the off-state.

4.1.2.3.2 On-state

When the external electric fields are applied to the two waveguides (on-state), the refractive index of the polymer in the two, low height, waveguides changes. This changes the effective refractive indices of the even and odd modes. Consequently, the

power splitting ratio and the beating length changes. Figure 4.6 shows the change in polymer refractive index; as well as, Figure 4.7 shows the electric filed mode profile of the even and odd modes in the on-state. .

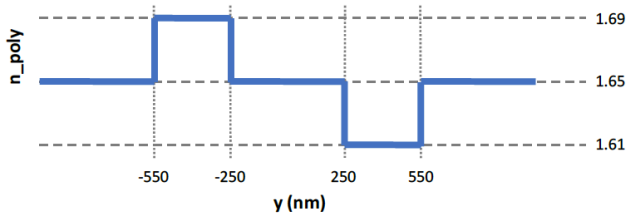

Figure 4.6 - The refractive indices of the polymer at the on-state.

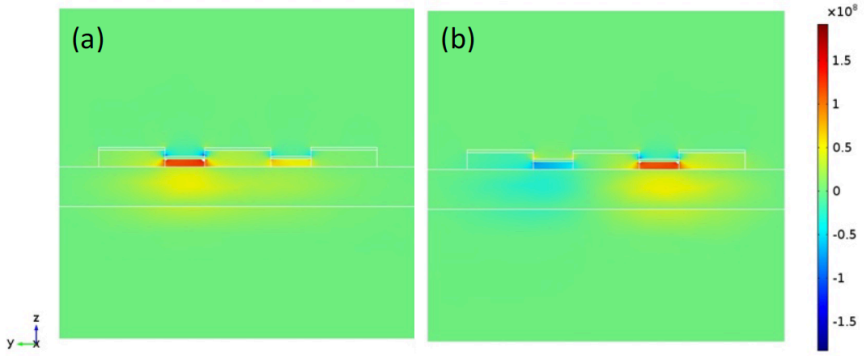

Figure 4.7 - The z-component of the field for (a) the even mode in the on-state, (b) the odd mode in the on-state.

4.1.3 Modulation properties of the electro-optic plasmonic directional coupler

The eigenvalue expansion method is used to study the coupling properties and the performance of the modulator. The modal excitation of the single waveguide port is excited. These waveguides can be easily excited using dielectric silicon waveguide [98]. This mode splits into two modes; then, their propagation along the directional coupler is monitored. At the off-state, the optical power couples from the first waveguide to the other waveguide at the coupling length l_c equals to 13 μm, as shown in Figure 4.8.

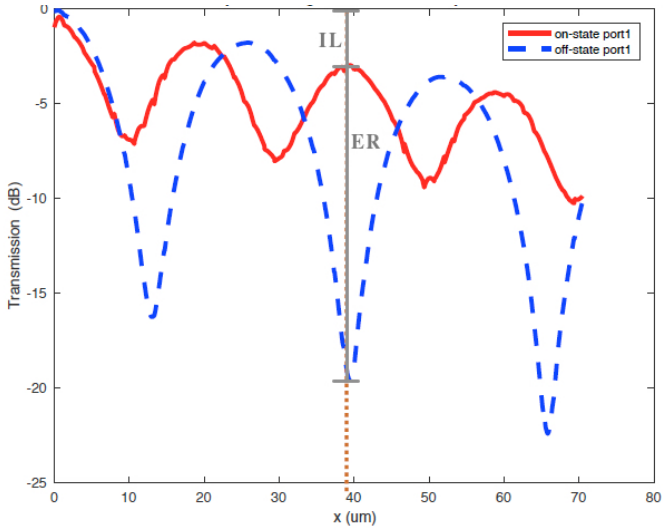

Figure 4.8 - channel 1 propagating power along the directional coupler for the off and on states of operation.

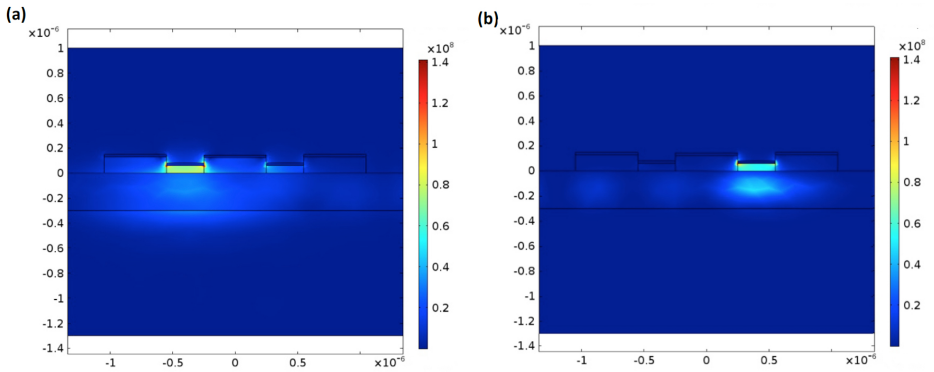

Figure 4.9 - The field profiles at a propagation distance equal to 3 Lc for (a) the on and (b) off state.

The propagation length for this modulator is chosen to be 3 L_c where the extinction ratio of the power at the first channel on the on-state to the off-state equals 14.34 dB. The insertion losses are estimated to be 2.298 dB.

The electric field needed to generate that change in the EOP refractive indices and respectively results in this extinction ratio are calculated. Then a positive voltage of 5.87 V should be applied between the metal (Ag) layer of the first waveguide and a negative voltage of 5.87 V should be applied to the metal layer of the second waveguide while keeping the Si layer grounded.

4.1.4 Conclusion

An organic electro-optical modulator based on hybrid-plasmonic directional coupler is studied and verified numerically using finite element tool. The power splitting

mechanism utilizes the Pockels effect of the polymer when an external electric field is applied. An extinction ratio of 14.34 dB and insertion loss of 2.298 dB are achieved at 39 μm modulator length. The level of the applied modulating voltage is calculated to be around 6 V.

Chapter 5 ITO based electro-optical modulators

ITO modeling

The active material used in the designs proposed in this chapter is indium-tin-oxide (ITO). Then, accurate description of the carrier accumulation is crucial before studying the modes.

Carrier density of the ITO can be utilized when used in MOS-structures [56]. ITO exhibits high electrical conductivity and has plasma frequency upon applying electrical (gate) voltage, which results in epsilon-near-zero (ENZ) effect [57], [58]. In other words, formation of this accumulation layer can tune plasma frequency and permittivity significantly.

The relative permittivity of the ITO can be described by the Drude model as in (5-1) [70]:

$$\epsilon_r = \epsilon_\infty - \frac{\omega_p^2}{\omega^2 - i\gamma\omega}; \tag{5-1}$$

where ϵ_∞ =3.9 F/m is the high-frequency dielectric constant, γ =1.8×10^{14} rad s^{-1} is the electron scattering rate, ω is the frequency of the light, and ω_p is the plasma frequency. The plasma frequency depends on electron concentration (n) and is defined as in (5-2) [99]:

$$\omega_p = \sqrt{\frac{ne^2}{\epsilon_0 m^*}}; \tag{5-2}$$

where $m^* = 0.35\ m_0$ is the electron effective mass in ITO, e is the electron charge, ϵ_0 is the permittivity of free space, and m_0 is the mass of electron.

The electron (carrier) concentration depends on the applied gate voltage (V_g) and the design. In the proposed design, the ITO layer is separated from the Si layer by a thin hafnium oxide (HfO_2) layer. The electron (carrier) concentration can be estimated by (5-3) [99]:

$$n_{acc} = n_0 + \frac{\epsilon_0 \cdot \kappa_{HfO_2} \cdot V_g}{e \cdot t_{HfO_2} \cdot t_{acc}}; \tag{5-3}$$

where $\kappa_{HfO_2} = 25$ is the DC permittivity of the HfO_2, $t_{HfO_2} = 5nm$ is the thickness of the HfO_2 layer (of our proposed designs). The accumulation layer thickness is assumed to be 1 nm, as in [99].

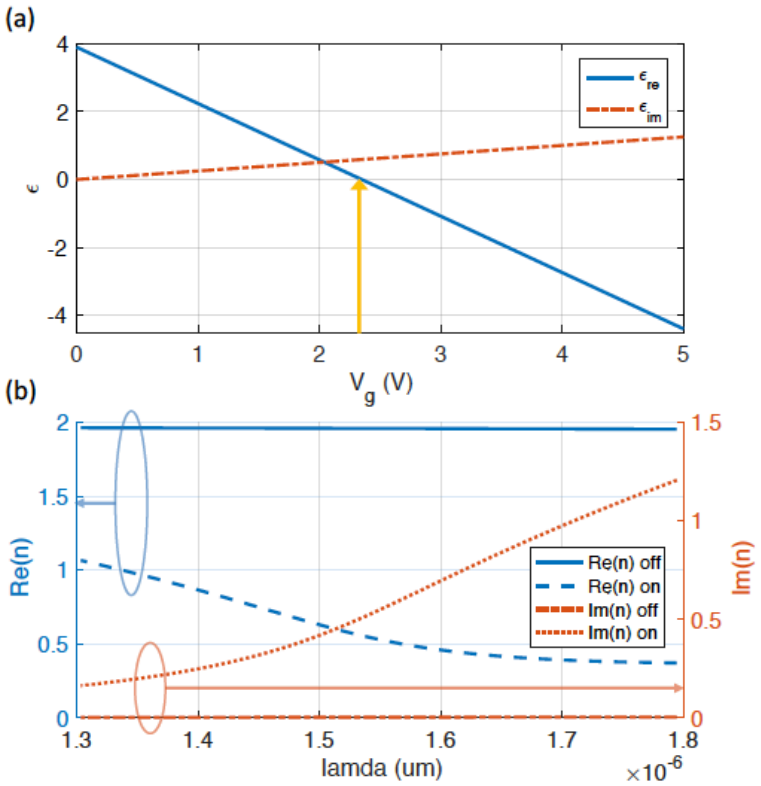

Figure 5.1 - (a) The complex permittivity of the ITO as a function of V_g at 1.55 µm (b) the optical properties of the ITO as a function of wavelength for the off- and on-states.

Using **Error! Reference source not found.** to **Error! Reference source not found.**, Figure 5.1(a) is plotted to show the relation between increasing V_g and the change in the complex permittivity of the ITO at 1.55 μm with the applied voltage (shows agreement with [73]). Increasing V_g leads to decreasing the real permittivity and increasing the imaginary permittivity of the ITO. At $V_g = 2.35V$, corresponding to $n_{acc} \cong 6.4\times10^{20}cm^{-3}$, the real permittivity reaches zero; thus, the ITO is considered an ENZ material. The ITO at this voltage acts as a metal instead of a dielectric. Figure 5.1(b) shows the optical properties of the ITO as a function of wavelength when there is no voltage applied (off-state) and when 2.35 V applied across the ITO (on-state) (shows agreement with [100]).

5.1 Design 2: Compact silicon electro-optical modulator using hybrid ITO tri-coupled waveguides[6]

Abstract

Silicon based electro-optical modulators are essential for optical communication systems. In this section, we present a silicon electro-optical modulator which is based on tri-coupled waveguides. Two of these waveguides are silicon-on-insulator slot waveguides separated by a hybrid Indium Tin Oxide intermediate waveguide. The silicon-on-insulator slot waveguides reaps the advantages of the high mode confinement. The power-splitting mechanism can be electrically tuned through applying external electric field to the intermediate plasmonic waveguide. The tuning mechanism is designed such that it will both change the coupling conditions and introduces additional intrinsic losses at the telecommunication wavelength (1550 nm). The modulator was optimized by 3D full finite difference time domain electromagnetic simulations. Extinction ratio of 6.14dB and insertion losses of 0.06 dB are realized at 21 μm modulator length; as well as, extinction ratio of 11.43 dB and insertion losses of 1.65 dB are realized at 34 μm modulator length. The proposed silicon electro-optical modulator can potentially play a key role in the next generation of the on-chip electronic-photonic integrated circuits.

5.1.1 Introduction

Over the past two decades, the demand increased for telecommunication network capacities and bandwidth. For example, in carrier networks, data traffic increases at a rate of 60% per year [6]. Also, the rising cloud-based computing is expected to increase the machine-to-machine data traffic by 90% per year [6]. Cisco forecasts data traffic to be 20.6 zettabytes per year by the year of 2021 [7]. To cope with this growing bandwidth demand, electronic baseband systems are replaced by optical broadband systems. Optical communication systems have many advantages, such as low cost, high bandwidth, and low transmission losses for long distances. In this scenario, modulation and switching are the principal operations in optical communication systems. High speed electro-optical modulators (EOMs) play a key role since they act as transistors in electronic circuits [6]. EOMs have many advantages, for

[6] Parts of this section were previously published in [C], other parts are under the submission to [E].

on-chip and off-chip applications, such as high bandwidth, low-loss transmission, and robustly resistant to external electromagnetic interference. Besides the technical characters, compatibility with the existing standard CMOS-VLSI technology must be considered. Modern optical communication systems are moving towards integrating dense EOMs to reduce both the energy consumption and the cost.

External optical modulation process involves controlling the optical properties of the optical carrier signal, such as amplitude, with a modulating information signal. Some external modulation techniques have been proposed utilizing electro-absorption and electro-optic (EO) effects [101]. Linear electro-optic effect (Pockels effect), is not found in silicon (Si) due to its centro-symmetric crystal structure [12]. Free carrier concentration change effect is the most important modulation mechanism affecting the real and imaginary parts of the refractive index of Si [12]. Carrier concentration change effect, known as plasma dispersion effect, is classified as electro-absorption mechanism. This mechanism exploits changes in the density of the free-carriers in the semiconductor material to modulate the real and imaginary parts of its refractive index [35].

Electrical inducing of the carriers can be through the field effect formation in metal-oxide-semiconductors (MOS) structures [102]. So far, many Silicon-Based EOMs have been developed based on carrier concentration change effect including, but not limited to, Mach–Zehnder interferometers (MZI), ring resonators, and metal-oxide-semiconductor capacitors [13]–[18]. Although modulators based on MZIs are promising in terms of modulation speed and optical bandwidth, they suffer from the large device footprints. While modulators based ring resonators have very narrow bandwidth [19]. To overcome these drawbacks, different designs have been studied [16], [20]–[24]. However, the speed of these devices is limited due to the lifetime of the carriers which is in the range of 1 GHz –10 GHz [6].

This raised the necessity for investigating other novel alternative materials [20], [30], [34]–[37]. Transparent conducting oxides (TCOs) are very promising because they are CMOS compatible. Indium-tin-oxide (ITO) is the most widely used TCO. The variation in free-carrier concentration renders the tunability of the ITO's electrical and optical properties [102]. Integrating ITO as the plasmonic material for EOMs attracted a lot of research due to its wide bandwidth and high thermal stability [34]. Yet, it suffers

from high insertion losses due to strong field enhancement in the lossy plasmonic waveguide.

To reduce the absorption propagation losses of the ITO-based waveguides without sacrificing bandwidth and modulation depth, the plasmonic ITO waveguide is used as intermediate coupler between the two main propagation slot waveguides. The slot waveguides will highly confine the optical power [103], [104]. The plasmonic intermediate waveguide can perturb the coupling environment and introduces losses as the optical power couples from one waveguide to the other. Another advantage of this design is that using a thin layer of ITO as the plasmonic material for the intermediate waveguide will produce high extinction ratio (ER) while limiting the capacitance. The goal is to reduce the overall capacitance of the device to reduce the power consumption and to increase the modulation speed.

In this section, an electro-optic modulator based on tri-coupled waveguides is introduced. Two of these waveguides are based on slot waveguides which support symmetric and anti-symmetric modes; these two waveguides are separated by a plasmonic, ITO-based, intermediate waveguide. The effective refractive index of the slot waveguide can be matched to the effective refractive index of the plasmonic coupler. This can be achieved at different dimensions so that different outcomes can be realized based on this structure. The power splitting mechanism of the modulator is based on changing carrier density in the ITO layer of the plasmonic waveguide by applying external electric field that changes the refractive index of the modes and attenuates the power. A finite difference time domain (FDTD) tool with a perfect matching layer (PML) boundary conditions is used to simulate and calculate the insertion losses, propagation losses, and extinction ratios [105]. We realized two designs: 1) 6.14 dB ER for 21 μm length of the modulator and 2) 11.43 dB ER for 34 μm length of the modulator.

In the next section, the properties of the active layer (ITO) will be presented; in section III, the structure and operating principle of the modulator will be introduced. In section IV, modulation properties of the electro-optic hybrid plasmonic modulator will be discussed. Finally, a brief summary and concluding notes are conveyed.

5.1.2 Design and operation principle

The proposed structure coupler is based on two slot waveguides which are separated by an ITO-based plasmonic waveguide. The design is shown in Figure 5.2.

The dimensions of the plasmonic waveguide can be adjusted, so the effective refractive index of the propagating mode, when no external electric field applied, matches the effective refractive index of the slot modes in the slot waveguides. This gives the environment for the power to couple back and forth from one slot waveguide to the other slot waveguide.

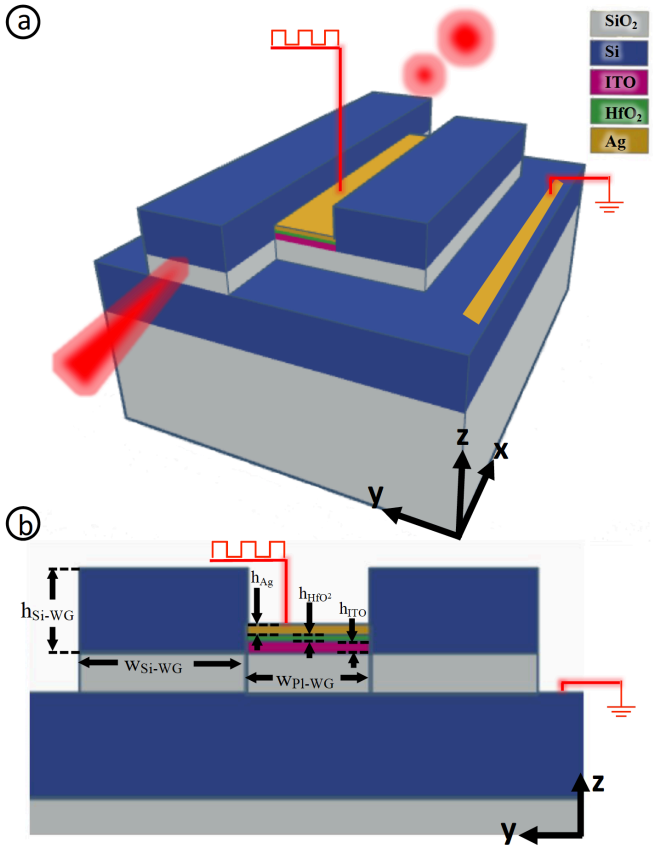

Figure 5.2 - (a) Schematic layout (Bird's eye view) and (b) cross-sectional of the proposed electro-optic modulator.

This can be fabricated by depositing SiO_2 on the top of silicon-on-insulator standard wafer. Another Silicon wafer is then bonded on top of the SiO_2 layer [106]. Mask is then used to etch Silicon over the middle coupler. Subsequently, a film is deposited to cover the whole wafer and then masks are used to pattern ITO, HfO_2 and silver layers.

5.1.2.1 Modal analysis

A commercial-grade simulator eigenmode solver and propagator was used to study the slot waveguide and the plasmonic intermediate coupler [107]. Also, it was

used to adjust the dimensions so that the effective refractive index of the slot mode matches the effective refractive index of the propagating mode of the plasmonic coupler when there is no external electric field applied.

5.1.2.1.1 Slot waveguide

The slot waveguide consists of a 70 nm of SiO_2 layer sandwiched between two 300 nm layers of silicon. The width of the slot waveguide $W_{Si\text{-}WG}$ = 400 nm. Electric field profile of the slot mode shows that the light is confined in the SiO_2 layer as shown in Figure 5.3(a). The refractive indices of the SiO_2 and Si at the telecommunication frequency are 1.444 and 3.476, respectively [108], [109].

5.1.2.1.2 ITO-based plasmonic waveguide

The plasmonic intermediate coupler consists of 70 nm height of SiO_2 layer topped with a 10 nm layer of ITO and 10 nm layer of silver (Ag). The ITO layer is isolated from the Ag layer with a 5 nm layer of Hafnium oxide (HfO_2) dielectric material to keep the carriers at the ITO layer when applying electric field to the metal. The width of the plasmonic coupler $W_{Pl\text{-}WG}$ = 300 nm. The refractive indices of the HfO_2 and Ag at the telecommunication frequency are 1.980 and 0.14447+11.366i, respectively [110], [111]. The ITO was defined using the model described earlier in section II. Figure 5.3 shows the electric field mode profiles for the propagating modes (b) when there is no external electric-field applied to the waveguide and (c) when there is an external electric-field applied.

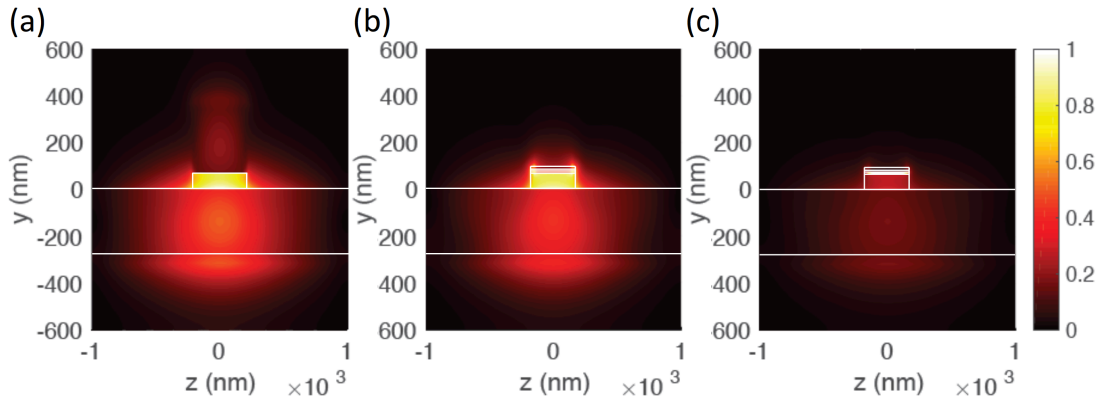

Figure 5.3 - (a) Field distribution (|Ez|) of the slot mode for width 400 nm. Field distribution (|Ez|) for the propagating modes of the plasmonic waveguide for width 300 nm: (b) off-state and (c) on-state.

When there is no external electric-field applied to the coupler (off-state), the electric field is confined in the SiO_2 layer as shown in Fig. 3(b). When there is an external electric-field applied to the coupler (on-state), the electric field is confined in the ITO layer due to the formation of an accumulation layer at the ITO- HfO_2 interface.

The effective refractive indices and the propagation losses of these two modes are listed in Table 5-1. The propagation losses of the on-state are much higher than the propagation losses of the off-state state due to the introduced plasmonic effects.

Table 5-1 Effective Refractive Indices And The Propagation Losses For The Modes Of The Plasmonic Waveguide.

Mode	Effective refractive index	Propagation loss (dB/μm)
Off-state	2.602	0.047
On-state	2.563	1.258

5.1.2.2 Modulator structure and principle of operation

Changing the dimensions of both the slot waveguide and the plasmonic coupler changes the effective refractive index of the modes of each waveguide. Varying the widths can slightly change the effective refractive indices. The height of the SiO_2 layer is optimized so that the effective refractive index of the slot waveguide is approximately similar to the effective refractive index of the off-state mode of the plasmonic coupler. The effective refractive indices can be exactly matched by changing the widths. Figure 5.4 shows the effective refractive indices for the slot mode of the slot waveguide and the off-sate mode of the plasmonic waveguide versus the width of each waveguide.

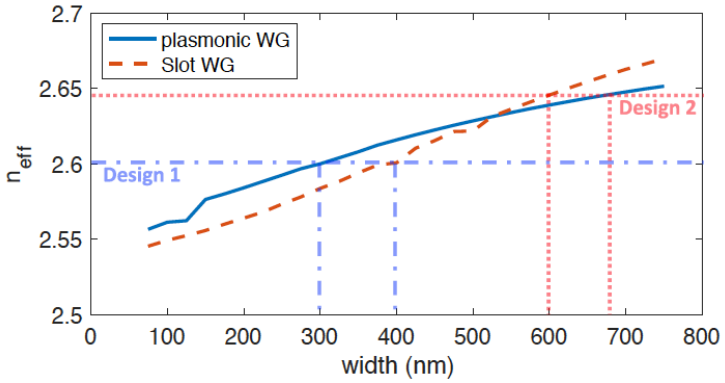

Figure 5.4 - The effective refractive index of the slot mode and plasmonic (off-state) mode vs. width of the waveguide. The dashed lines indicate the dimensions for the two designs.

5.1.2.2.1 Off state

The plasmonic coupler is placed between the two slot waveguides. When there is no external electric field applied to the middle (plasmonic) coupler, the effective refractive indices of the two slot waveguides and the plasmonic coupler are almost the same. This results in two modes, even (symmetric) and odd (anti-symmetric) modes. Figure 5.5 shows the z -component of the electric field for the symmetric and the anti-symmetric modes when there is no electric field applied over the middle waveguide.

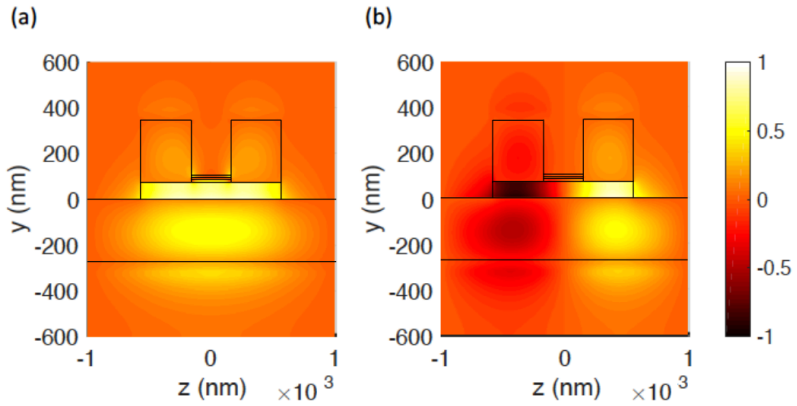

Figure 5.5 - Field distribution (|Ez|) for (a) the even and (b) the odd mode in the off-state.

5.1.2.2.2 On state

Applying electric field over the intermediate coupler accumulates free-carriers at the ITO-HfO_2 interface which results in confining the electric field in the ITO layer. This changes the effective refractive indices and the losses of the even and odd modes. Consequently, it affects the length of the modulator. Figure 5.6 shows the z -component

of the electric field for the symmetric and the anti-symmetric modes when there is electric field applied over the middle waveguide.

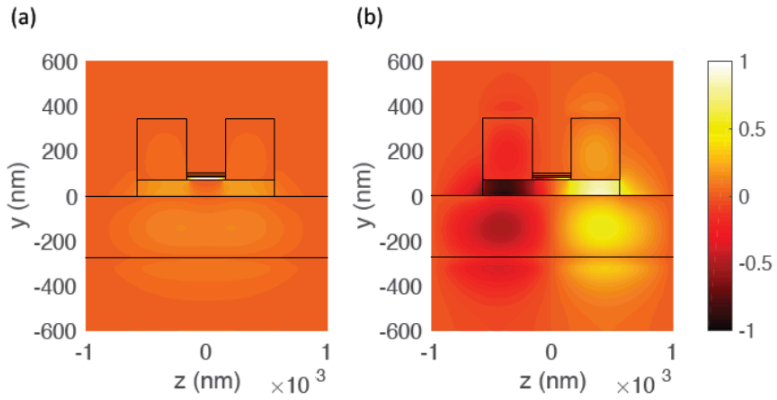

Figure 5.6 - Field distribution (|Ez|) for (a) the even and (b) the odd mode in the on-state.

Table 2 summarizes the properties of the even and odd modes for the off- and on-states. Additionally, overlap analysis is performed to calculate the power coupling between these modes and the input mode, exciting the slot mode through one of the slot waveguides (input waveguide). The results for this analysis are also included in Table 5-2.

Table 5-2 - Comparison between the even and odd modes for the off- and on-states.

State	Mode	Effective refractive index	Propagation loss (dB/μm)	Power coupling from the input mode
Off-state	even	2.652	0.0036	77.1
	odd	2.556	0.0004	19.8
On-state	even	2.644+0.0157i	0.5549	77.2
	odd	2.555+0.0017i	0.0620	19.6

5.1.2.2.3 Principle of operation

The modal excitation of the modulator is done by exciting the slot mode through the input waveguide (extended waveguide). Such waveguide can be excited using dielectric silicon waveguide [98]. The power couples from one of the slot waveguides to the other passing through the middle plasmonic coupler. Once the electric field is applied over the middle coupler, the propagation losses increase. Thus the power couples from one arm to the other will decrease and the coupling length will change. Moreover, the power is not confined in the SiO_2 layer, which also decreases power coupling between the two arms.

Figure 5.7 shows electric field intensity, with respect to the input intensity, at the center of the SiO_2 layer of the input waveguide along the propagation length when there is no voltage and with applied voltage across the middle coupler.

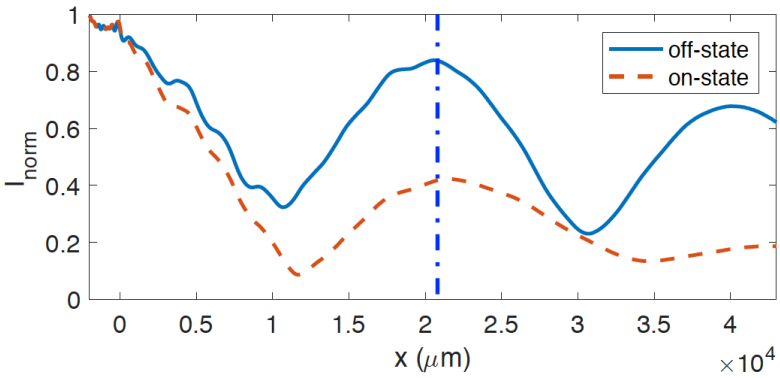

Figure 5.7 - The normalized intensity, with respect to the input, of the guided mode at the center of the SiO2 layer of the input waveguide as a function of the propagation length for the off- and on-states, for D1. The dashed line indicates the length for D1.

5.1.3 Modulation properties of the electro-optic modulator

As shown in Figure 5.4 matching between the effective refractive indices for the slot mode of the slot waveguide and the off-sate mode of the plasmonic coupler at different widths can be achieved. Therefore, different designs can be realized based on this structure. In this section we studied all the aspects for $W_{Si\text{-}WG}$ = 400 nm and $W_{Pl\text{-}WG}$ = 300 nm (D1). Matching the effective refractive indices at different widths will change the effective refractive indices of the even and odd modes, the power coupling from the input mode, and the propagation losses. Thus, the length of the modulator as well as the extinction ratio will differ.

The relation between the widths of the waveguides and the modulation properties is studied. Firstly, increasing the widths will reduce the power coupling between the input mode and the even mode and consequently increases the coupling with the odd mode. This also reduces the difference between the even and the odd modes. Thus, the length of the modulator coupler increases. However, increasing the length of the modulator increases the extinction ratio. Secondly, reducing the widths, beyond 300 for the plasmonic waveguide and 400 for the slot waveguide, most of the power will couple to the even mode and it does couple to the other waveguides. The power mainly propagates in the input waveguide and small portion dissipates to the other two waveguides. Another design is also studied, $W_{Si\text{-}WG}$ = 600 nm and $W_{Pl\text{-}WG}$ = 675 nm

(D2). This design achieves around 50% coupling to the even mode and 50% coupling to the odd mode.

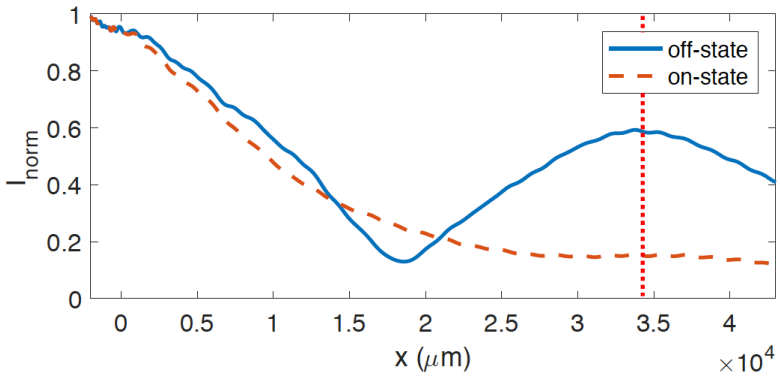

Figure 5.8 - The normalized intensity, with respect to the input, of the guided mode at the center of the SiO2 layer of the input waveguide as a function of the propagation length for the off- and on-states, for D2. The dashed line indicates the length for D2.

Figure 5.7 and Figure 5.8 were used to optimize the modulator length that results in maximum extinction ratio. From Figure 5.7, the length of the modulator is 21 μm (~ coupling length) for D1. Similarly, from Figure 5.8, the length of the modulator is 34 μm for D2. A commercial-grade simulator based on the finite-difference time-domain method was used to calculate the insertion losses, and extinction ratios at the modulation length [112].

5.1.3.1 Insertion loss

The results for the insertion losses (IL) for both designs are shown in Figure 5.9. At 1.55 μm, the IL are 0.06 dB and 1.65 dB for D1 and D2, respectively.

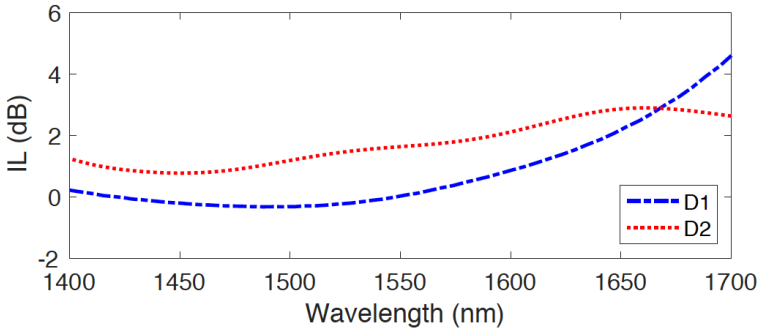

Figure 5.9 - Insertion losses of both designs as function of wavelength.

5.1.3.2 Extinction ratio

Extinction ratio (ER) is the most important parameter for the modulator since it is the ratio between the power at the output port at the off-state to that at the on-state. Figure 5.10 shows the results for the ER for both designs as a function of wavelength. The ER for D1 is 6.1 dB and for D2 is 11.43 dB, at the operating wavelength (1.55 μm).

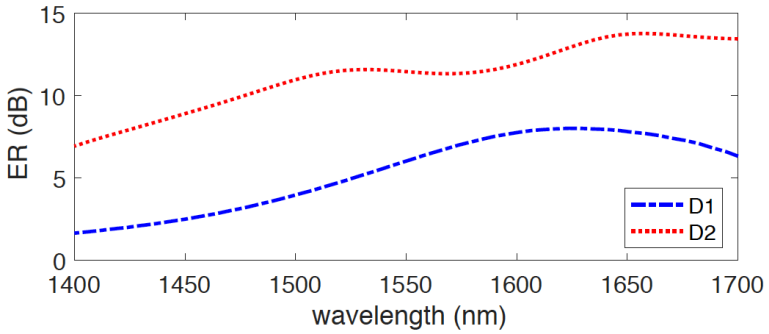

Figure 5.10 - Extinction ratio of both designs as function of wavelength.

Previous results are based on 2.35 V applied across the ITO plasmonic waveguide. Digital modulation can be realized by plotting ER versus the modulation voltage. Changing the applied voltage changes the ER as shown in Figure 5.11 at the operating wavelength (1.55 μm). The ER is saturating above 2.35. Digital modulation is confirmed based on the steep slope and the saturation effect that split ER into two distinguishable states; a transparent transmitting state at low voltages (below 1.5 V) and an absorbing saturating state above 2.35 V.

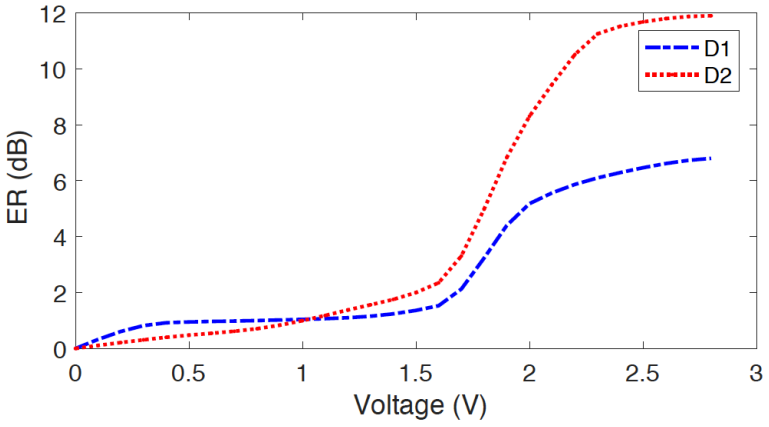

Figure 5.11 - Extinction ratio of both designs as function of the applied voltage at 1.55 µm.

5.1.3.3 Energy consumption and modulation speed

The modulation speed of any optical modulator is related to the capacitance and resistance of the device. Capacitance and the modulation voltage are related to energy consumption. The modulation speed limit is defined as $f_{max}=(2\pi RC)^{-1}$. The energy consumption per bit can be estimated using E/bit = $(CV^2)/2$.

Electrostatic RC analysis, performed with finite element method using a commercial solver, was used to calculate the capacitance C of the intermediate plasmonic coupler as 33.6 fF for D1 and 11.4 fF for D2 [113].

The applied voltage is 2.35 V and the resistance of the device is assumed to be 100 Ω, including the interconnects. This yields to $f_{max} \approx$ 47.5 GHz for D1 as well as $f_{max} \approx$ 140 GHz for D2. Furthermore, E/bit = 67.1 fJ/bit for D1 and E/bit = 22.7 fJ/bit for D2. Figure 5.12 shows the distribution of the electric field in the dielectric and air domain surrounding the intermediate plasmonic coupler.

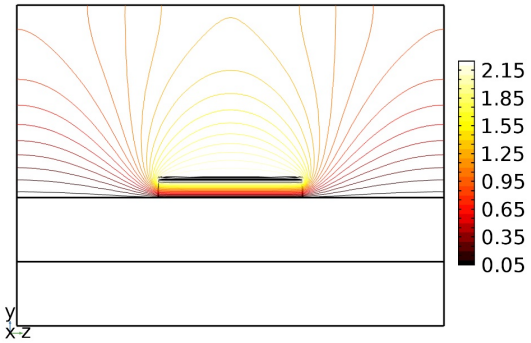

Figure 5.12 - Electrostatic potential contours in the dielectric and air domain surrounding the intermediate plasmonic coupler.

5.1.3.4 Summary

Table 5-3 summarizes the modulation properties of the two designs.

Table 5-3 - Summary of the modulation properties for both designs at the operating wavelength.

Design	Length of the modulator (μm)	Insertion loss (dB)	Extinction ratio (dB)	f_{max} (GHz	E/bit (fJ/bit)
-·-·- D1	21	0.06	6.14	47.5	67.1
····· D2	34	1.65	11.43	140	22.7

5.1.4 Conclusion

A low insertion loss compact silicon electro-optic modulator is studied, using a finite difference time domain method with perfect matching layer (PML) absorbing

boundary conditions. The modulator is based on two silicon slot waveguides separated by an ITO based plasmonic waveguide. The power tuning mechanism is based on carrier accumulation at the ITO-dielectric interface through applying external electric field. To employ Drude model, the real part of the permittivity of the ITO layer, which can reach zero (epsilon-near-zero ENZ effect) by electrical tuning of the carrier accumulation layer, is verified. Thus, optical power experiences attenuation as it propagates along the modulator. Different designs can be realized based on this design. 6.14 dB ER and 0.06 dB IL realized at 21 μm modulator length. 11.43 dB ER and 1.65 dB IL realized at 34 μm modulator length. Electrical voltage of 2.35 V is applied to the plasmonic coupler. The devices show satisfactory performance in terms of extinction ratio and foot print. Also, broadband operation of this modulator is promising. Such hybrid silicon-on-insulator modulators offer bridging existing electronic and photonic platforms. A new stages of integration will ultimately set.

5.2 Design 3: High-speed hybrid plasmonic electro-optical absorption modulator exploiting epsilon-near-zero effect in ITO[7]

Abstract

Using transparent conducting oxides (TCOs), like indium-tin-oxide (ITO), for optical modulation attracted research interest because of their epsilon-near-zero (ENZ) characteristics at telecom wavelengths. Utilizing indium-tin-oxide (ITO) in multilayer structure modulators, optical absorption of the active ITO layer can be electrically modulated over a large spectrum range. Although they show advances over common silicon electro-optical modulators (EOMs), they suffer from high insertion losses. To reduce insertion losses and device footprints without sacrificing bandwidth and modulation strength, slot waveguides are promising options because of their high optical confinement. In this section, we present the study and the design of an electro-optical absorption modulator based on electrically tuning ITO carrier density inside a MOS structure. The device structure is based on dielectric slot waveguide with an ITO plasmonic waveguide modulation section. By changing the dimensions, the effective refractive indices for the slot mode and the off-sate mode of the plasmonic section can be matched. When applying electric field to the plasmonic section (on-state), carriers

[7] Parts of this section were previously published in [D], other parts are under the submission to [F].

are generated at the ITO-dielectric interface that result in changing the layer where the electric field is confined from a transparent layer into a lossy layer. A finite difference time domain method with perfect matching layer (PML) absorbing boundary conditions is taken up to simulate and analyze this design. An extinction ratio of 15.5 dB is achieved for a 10-μm-long modulation section, at the telecommunications wavelength (1.55 μm). This EOM has advantages of simple design, easy fabrication, compact size, compatibility with existing silicon photonics platforms, as well as broadband performance.

5.2.1 Introduction

Optical modulators are very vital to silicon photonics, as they provide a bridge between the photonic world and the digital electronic world [114], [20]. Electro-optical modulation includes controlling the amplitude, polarization and/or phase of the optical signal with a modulating electrical signal [115]. There are many techniques for optical modulation such as electro-optic (EO), electro-absorption, and thermo-optic effects [6], [23].

The carrier concentration change effect is classified as electro-absorption mechanism. Alternatively called plasma dispersion effect, this mechanism controls the concentration of the free electrons and holes in semiconductor materials to control the real and imaginary parts of their permittivity [116]. This effect in silicon limits the modulation speed due to the lifetime of the carriers which is in the range of 1 GHz –10 GHz [6]. Thus, the demand raised for investigating new plasmonic materials with larger linear and non-linear optical properties. Transparent conducting oxides (TCOs) are among the materials investigated for modulation applications [24], [37], [61], [62], [86], [100], [103].

TCOs are very encouraging because of their CMOS compatibility. Having plasma frequency close to the telecommunication wavelengths, TCOs are very suitable for modulation applications in the near infrared (NIR) [24], [40], [74], [117], [118]. This means that changes in the carrier accumulation strongly affect the optical properties of the TCOs [58], [71]. Also, carrier accumulation processes in the TCOs are ultrafast; electro-optical modulators based on TCO as the plasmonic material offer modulation speeds in the range of THz [34], [75].

Using Indium-tin-oxide (ITO), the most known TCO, as the plasmonic material attracted the attention because of its high bandwidth [24]. Though, strong field enhancement in the lossy ITO based waveguide contributes to high insertion loss.

A reliable EOM should have a small footprint, high speed, high extinction ratio (ER), low insertion loss (IL) and low energy consumption. ITO based plasmonic absorption modulators have been suffering from a critical trade-off between the modulation speed and insertion loss [24], [34], [117], [119]. To reduce the insertion loss while maintain high modulation speed, in this section, we introduce an ITO based plasmonic absorption modulator built on slot waveguide structure. The modulator is based on silicon on insulator slot waveguide with an ITO based plasmonic modulation section. Slot waveguide structure of the modulator is promising because of its high optical confinement, resulting in low insertion loss. The modulation mechanism is based on changing carrier density in the ITO layer of the plasmonic section by applying external electric, changing the refractive index of the modes and attenuating the power. A finite difference time domain (FDTD) tool is used to investigate the optical properties of the proposed modulator [105]. An ER of 15.49 dB and IL of 1.01 dB were realized for 10 μm length of the modulation section. The speed of the device is in the range of gigahertz; the energy consumption is also in the range of femto-joule per bit.

5.2.2 Device structure

5.2.2.1 Device layout

The proposed design is based on slot waveguide. The input and the output ports are standard silicon on insulator slot waveguides. The modulation section is an ITO-based slot hybrid plasmonic waveguide. The design is shown in Figure 5.13.

This device be fabricated by depositing a layer of SiO2 on the top of silicon-on-insulator standard wafer. Then, additional Silicon wafer is bonded on top of the SiO2 layer [106]. Mask is then used to etch Silicon over the modulation section. Afterwards, a film is deposited covering the whole wafer and then masks are used to pattern ITO, HfO2 and silver layers over the modulation section.

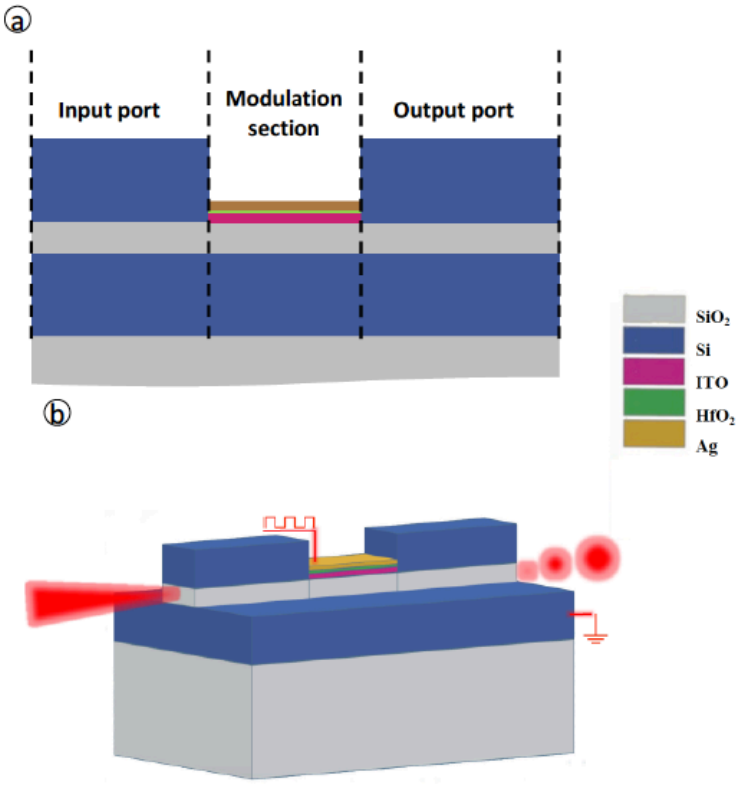

Figure 5.13 - (a) side view and (b) Schematic layout (Bird's eye view) of the proposed electro-optical absorption modulator.

5.2.2.2 Modal analysis

The refractive indices of the Si, SiO_2 and HfO_2 are 3.47, 1.44 and 1.98, respectively. The refractive index of the ITO calculated through wavelength-dependent model described earlier. An Eigen mode finite difference solver is used to study the slot waveguide and the modulation plasmonic section. Also, it is used to match the effective refractive index and the width of the slot waveguide and the modulation section.

The slot waveguides consist of a 70 nm of SiO2 layer sandwiched between two 300 nm layers of silicon. The electric-field is confined in the SiO2 layer as shown in Figure 5.14(a). This mode has approximately no propagation losses.

This section consists of 70 nm of SiO2 layer topped with a 10 nm layer of ITO and 10 nm layer of silver (Ag). The ITO layer is isolated from the Ag layer with a 5 nm layer of Hafnium oxide (HfO2) dielectric material to keep the carriers at the ITO layer when applying electric field to the metal.

At the off-state, when there is no electric field applied, the mode is confined in the SiO2 layer as shown in Figure 5.14(b). When an external electric field is applied to the

modulation section, on-state, the mode is confined on the ITO layer, as shown in Figure 5.14(c), due to the accumulation of free carriers at ITO- HfO2 the interface.

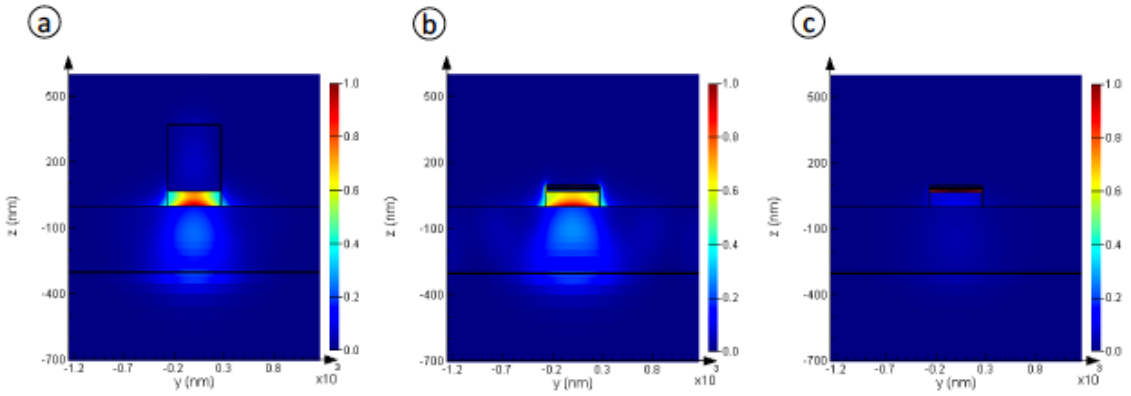

Figure 5.14 - (a) Field distribution (|Ez|) of the slot mode. Field distribution (|Ez|) of the plasmonic section modes: (b) off-state and (c) on-state.

The effective refractive indices and the propagation losses of these modes are listed in Table 5-4.

Table 5-4 - Effective refractive indices and the propagation losses for the modes.

Mode	Effective refractive index	Propagation loss (dB/μm)
Slot mode	2.632	~ 0
Plasmonic mode: off-sate	2.632	0.029
Plasmonic mode: on-sate	2.598	1.854

5.2.2.3 Optimization

To minimize the coupling losses, from input and output ports to the modulation plasmonic section, the effective refractive index and the width were matched. This also minimizes the overall insertion losses of the modulator. Figure 5.15 shows the effective refractive indices for the slot mode of the slot input/output ports and the off-sate mode of the plasmonic modulation section versus the width of each waveguide. The width of the modulation adjusted to be 525 nm.

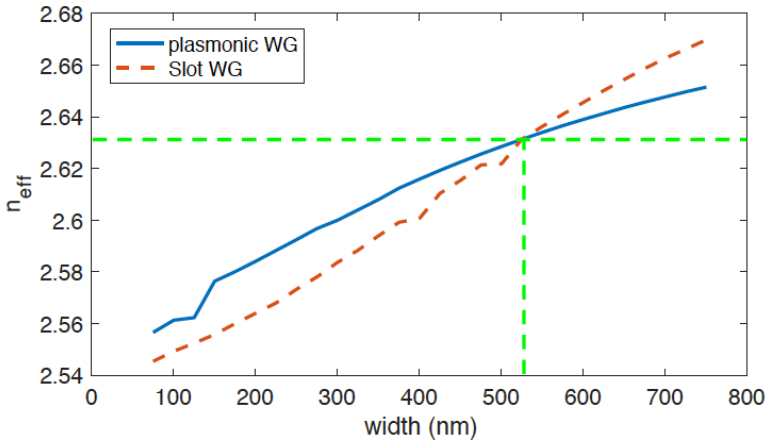

Figure 5.15 - The effective refractive index of the slot mode and plasmonic (off-state) mode vs. width of the waveguide.

5.2.3 Principle of operation

The excitation of the modulator is through exciting the slot mode in the input port. The power propagates through the slot waveguide till it reaches the modulation section. Since, the effective refractive index of the slot waveguide matches that of plasmonic modulation section, most of the power couples to the modulation section and propagates through the SiO_2 layer. This results in very small insertion losses of the whole modulator.

When an external voltage applied to the modulation section, an accumulation layer is formed at the ITO- HfO2 interface. Increasing the applied voltage decreases the real permittivity and increases the imaginary permittivity of the ITO. Using Drude model, the change in the real and imaginary permittivities of the ITO can be predicted [56]. When the applied voltage reaches 2.35 V, corresponding to electron (carrier) concentration of 6.4 x 10-20 cm-3, the real permittivity of the ITO reaches zero; accordingly, the ITO is considered an epsilon-near-zero material.

Consequently, the power that couples from the input port to the modulation section propagates through the ITO layer which results in less coupling. Also, applying external electric field to the ITO-based modulation section introduces additional intrinsic losses.

5.2.4 Results and Modulation properties

Finite difference time domain simulations, with perfect matching layer (PML) absorbing boundary conditions, were carried out to simulate and analyze this design. An

ER of 2.3 dB and IL of 0.69 dB are achieved for a 1-μm-long modulation section, at the telecommunications wavelength (1.55 μm). Increasing the length of the modulation section increases the ER significantly. The ER and IL for different modulation section lengths are listed in Table 2. A figure of merit (FOM) should be described to evaluate the modulation performance. We defined FOM as the ratio between the ER and IL as $FOM = ER/IL$. Also, FOM for different modulation section lengths is listed in Table 5-5. Figure 5.16 shows the normalized mode intensity, with respect to the input intensity, at the center of the SiO_2 layer of the input waveguide along the propagation length when there is no voltage and with applied voltage across the modulation section. IL and ER as function of wavelength are shown in Figure 5.17 for the 10-μm-long modulation section.

Table 5-5 - IL, ER, and FOM for different modulation section lengths.

Length of the modulator (modulation section) (μm)	IL	ER	FOM
1	0.69	2.3	3.34
2	0.74	4	5.43
3	0.75	5.64	7.49
5	0.77	8.56	11.02
10	1.01	15.49	15.34

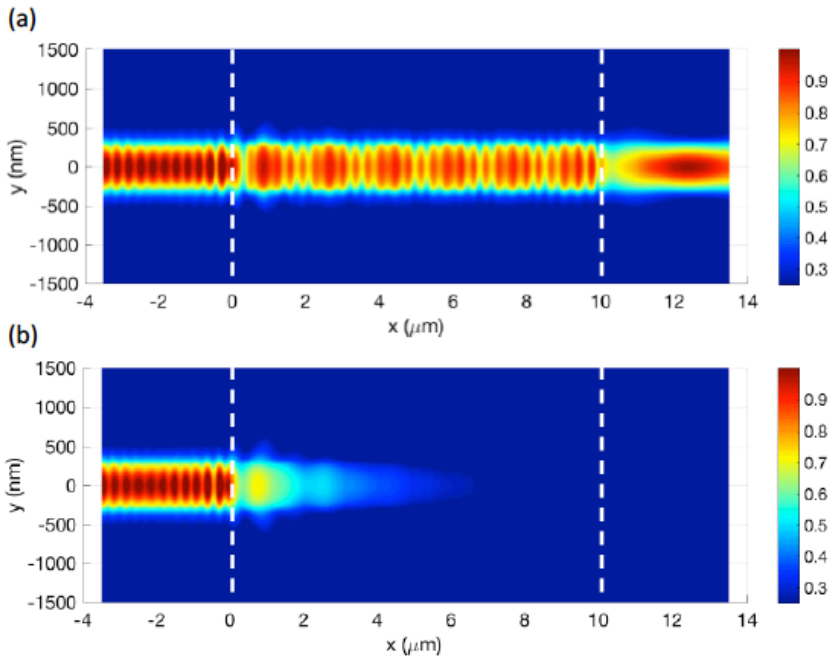

Figure 5.16 - The normalized intensity, with respect to the input, of the guided mode at the center of the SiO2 layer for (a) off- and (b) on-states. The dashed lines indicate the modulation section.

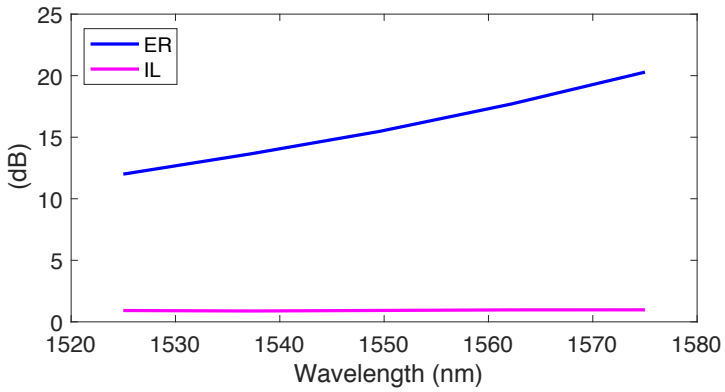

Figure 5.17 - IL and ER as a function of wavelength.

The modulation speed is related to the capacitance and the resistance of the modulator as the modulation speed limit is defined as $f_{max} = (2\pi RC)^{-1}$. Also, energy consumption is related to the capacitance and modulation voltage as the energy consumption per bit can be calculated using $\mathrm{E/bit} = CV^2/2$. Electrostatic RC analysis carried out with finite element method using a commercial solver, to calculate the capacitance of the modulation section. The capacitance for the 10 μm long modulation section is found to be 2.64 fF. The resistance of the modulator is assumed to be 100 Ω. This lead to $f_{max} \approx$ 600 GHz and E/bit = 7 fJ/bit.

5.2.5 Conclusions

An electro-optical absorption modulator based on ITO's ENZ effect is studied. The design and the principle of operation are described. Modal and FDTD analysis were performed to verify and simulate the design. An extinction ratio of 15.49 dB and an insertion loss of 1.01 dB can be achieved for 10 μm long modulation section. The design shows satisfactory results in terms of extinction ratio, insertion loss, foot print, and energy consumption. Also, this modulator has a potential for broadband operation due to the nonexistence of resonance effect. Such silicon-on insulator electro-optical modulators, with high extinction ratios, insertion losses, and low energy consumptions, are fundamental for bridging photonic platforms to the existing electronics.

5.3 Ring resonator based on this design

Trials to construct a ring resonator modulator based in this design were performed. The input and the output waveguide are the slot waveguide, described in the previous sections, and the ring resonator is based on the ITO slot plasmonic waveguide, described in the previous sections. The trials showed that the ITO slot plasmonic waveguide is very lossy for a ring design.

Another trials performed to study the ring resonator design based on the input and the output waveguide are ITO slot plasmonic waveguide, and the ring resonator is based on the slot waveguide. The trials showed that the slot waveguide cannot be implemented for ring resonator because its high bend losses.

Chapter 6 VO_2 based electro-optical modulators

Design 4: Hybrid plasmonic-vanadium dioxide electro-optical switch based modulator [8]

Abstract

This work presents the study and the design of optical switch based on a hybrid plasmonic-vanadium dioxide waveguide. The power-attenuating mechanism takes the advantage of the phase change properties of vanadium dioxide that exhibits a change in the real and complex refractive indices upon switching from the dielectric phase to the metallic phase. The proposed switch designed to operate under the telecommunication wavelength. The switch was analyzed by 3D full electro-magnetic simulations. An ER per unit length of 4.32 dB/μm and IL per unit length of 0.88 dB/μm are realized for the proposed electro-optical switch. The proposed electro-optical switch has the advantages of small device foot-print, compatible with the existing VLSI-CMOS technology and broadband operation.

6.1.1 Introduction

Optical communications have revolutionized the telecommunication industry. Nowadays, optical communication systems are taking over traditional electronic baseband systems, due to the numerous advantages such as high bandwidth, relatively low transmission losses for long distances, low cost, and robustness to external electromagnetic interference. Electro-optical modulators (EOMs) are indispensable components for integrating photonic circuits with existing electronic circuitries [6]. Current optical communication systems are focusing on integrating dense EOMs to reduce both the cost and the energy consumption.

All-silicon EOMs have been realized based on carrier concentration change effect including, but not limited to, Mach–Zehnder interferometers (MZI), ring resonators, and metal-oxide- semiconductor capacitors [13]–[15], [120]–[122]. Carrier concentration change effect, considered as electro-absorption mechanism, utilizes changes in carrier density to control the real and imaginary parts of the refractive index of silicon [35]. Designs based on MZIs are encouraging because of their wide bandwidth and high

[8] Parts of this section are submitted to [G].

modulation speeds. However, they have large footprints [123]. On the other hand, resonant EOMs have a very narrow bandwidth [123].

The main issue with all-silicon EOMs is that their modulation speed are limited to few gigahertz due to the lifetime of the carriers [120], [123]. Also, they are sensitive to the fluctuations in the ambient temperature [124]. EOMs with higher modulation speed and less sensitive to the temperature are proposed using III-V materials such as lithium niobate and gallium arsenide [125]. However, these materials are not compatible with the existing CMOS technology which hinders the integration for on-chip applications.

Hybrid structures have been proposed by combining silicon with other novel materials such as organic polymers, graphene, indium-tin-oxide (ITO), and vanadium dioxide (VO_2) [31], [69], [74], [81], [118], [126]–[128]. Such structures reap the advantages of overcoming silicon intrinsic limitations and maintaining CMOS compatibility.

Vanadium dioxide (VO_2), a phase change material, alters the real and complex refractive indices upon switching from the dielectric phase to the metallic phase [51]. VO_2 has been emerging as a noteworthy candidate to combine with silicon in photonic devices due to its phase change property [129]. At room temperature, VO_2 is in the insulator dielectric state. Its phase can be altered to a conductive metallic state. This insulator-metal phase change can be triggered thermally, optically, electrically, or mechanically on ultrafast time scales [130]–[137]. At the telecommunication wavelength (1.55 μm), its real refractive index drops from 2.86 to 1.66, and the imaginary part rises from 0.26 to 3.29 [138], [139]. This change in the refractive index is three to four order of magnitude higher than the maximum index change achievable by carrier concentration change effect is silicon. This feature enables designing optical modulators with high extinction ratio (ER) and small foot-print; however, the high absorption of VO_2 results in high insertion loss (IL) [79].

Plasmonics offer a parallel path for realizing compact and low power EOMs through the high field confinement at the interface between conductors and dielectrics [140], [141]. Howver, plasmonic EOMs suffer from high insertion losses. Hybrid Si-VO_2 optical switches have been demonstrated utilizing the surface plasmon polariton propagating at the interface between silver and VO_2 [81], [142]. Designing a hybrid

plasmonic-vanadium dioxide electro-optical modulator with high ER, low IL, and small footprint is very challenging.

In this paper, we propose an electro-optical switch based on silicon-on-insulator rib waveguide coated with VO_2 and metal layers. The optical wave is guided in the silicon layer. The refractive index of VO_2 changes with the applied electric field; that results in changes in the mode profile which affects the power transmission. The change in the VO_2 refractive index significantly changes the effective refractive index of the propagating mode as the mode changes from a photonic mode propagating in in the silicon layer to a plasmonic mode propagating at the Si-VO_2 interface. A finite difference time domain (FDTD) tool with a perfect matching layer (PML) boundary conditions is used to optimize, simulate and calculate the insertion losses, propagation losses, and extinction ratios [105]. An ER per unit length of 4.32 dB/μm and IL per unit length of 0.88 dB/μm are realized for the proposed electro-optical switch.

In the next section, the design is illustrated. In section 3, the principle of operation is discussed. The optimizations and the modulation properties of the proposed design are demonstrated, respectively, in section 4 and 5. Finally, in section 6, brief summary and concluding notes are delivered.

6.1.2 Design

The proposed hybrid absorption switch is based on silicon-on-insulator (SOI) rib waveguide. To modulate the optical power, the modulation section is formed by coating the SOI rib waveguide with VO_2 and metal layers as shown in Figure 6.1. The optical wave is guided in the Si-rib.

This design can be fabricated on silicon-on-insulator (SOI) standard wafer. A thick layer of silicon is etched; then, selective etching is used to form lower part of the rib waveguide. VO_2 layer is, then, vacuum-deposited coating the upper part of the Si-rib waveguide as shown in figure 1. Metal (silver) electrode was evaporated onto the surface of the VO_2 layer.

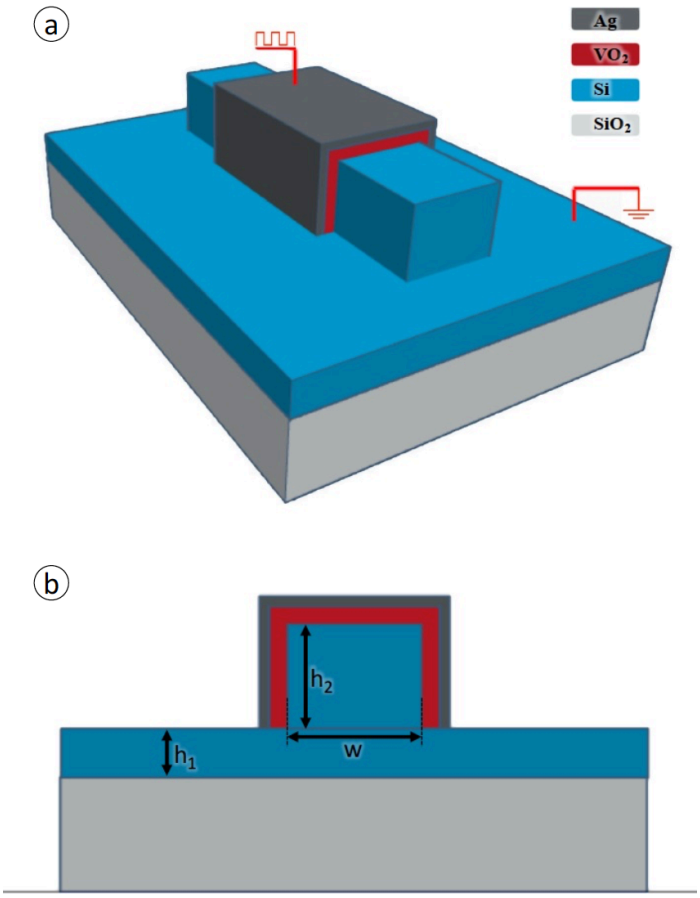

Figure 6.1 - Schematic layout of the proposed hybrid electro-absorption switch. (b) Cross section view of the electro-absorption switch.

6.1.3 Principle of operation

The optical wave is excited through the SOI-rib waveguide. In the off-state, when there is no external electric field applied to the modulation section is applied, the optical wave propagates through plasmonic modulation section with minor losses The metal layer above the VO_2 layer acts as metallic contact for applying the external electric field; the Si-rib waveguide is kept grounded. When an external electric field is applied to the metal layer, the VO_2 layer switches from the dielectric phase to the metallic phase. Thus, the effective refractive index of the propagating mode changes; as well as, the losses upturns. This results in perturbing the propagating power.

An Eigen mode finite difference solver is used to analyze the modes and calculate the losses [107]. The field distribution ($|E_z|$) of Si-rib input waveguide mode is shown in Figure 6.2.

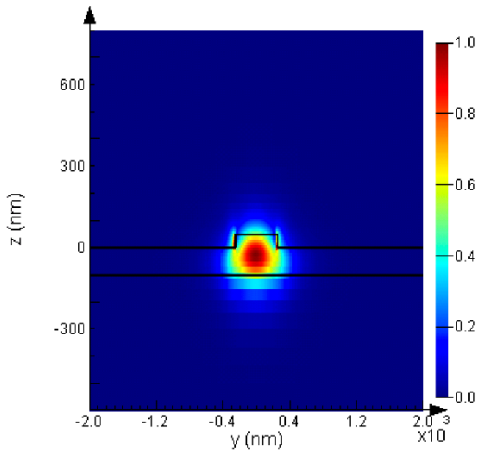

Figure 6.2 - Field distribution ($|E_z|$) of the input mode of the Si-rib waveguide.

The field distribution ($|E_z|$) of the modulation section modes, off-state and on-state, are shown in Figure 6.3. The effective refractive indices and the propagation losses of these modes are summarized in Table 6-1.

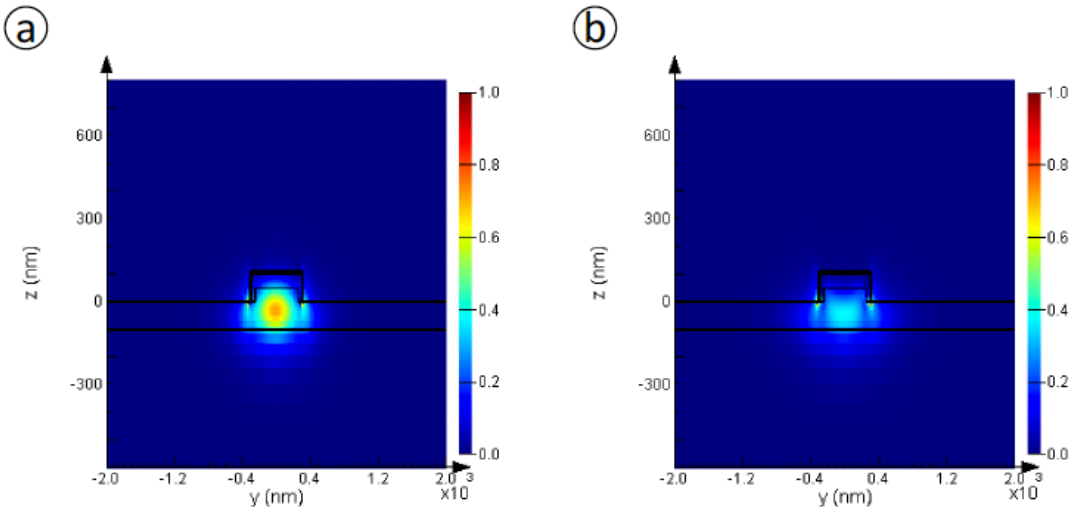

Figure 6.3 - Field distribution ($|E_z|$) of the propagating modes of the plasmonic modulation section: (a) off-state and (b) on-state.

Table 6-1 - Effective refractive indices and the propagation losses for the modes at 1.55 μM

Mode	Effective refractive index	Propagation loss (dB/μm)
Si-rib input mode	2.296	~ 0
Off-state modulation section	2.284	0.829
On-state modulation section	2.166	3.785

6.1.4 Device optimization

The main goal in designing an electro-optical modulator is 1) maximizing the extinction ratio (ER), 2) minimizing the insertion loss (IL) and 3) reducing the device foot-print. In the proposed design, three parameters (h_1, h_2, and w) need to be optimized.

Two dimensional modal analysis is used to optimize the dimensions by defining modal figure-of-merit (FOM_{modal}). FOM_{modal}, as described in (1), is defined as the ratio of the modal propagation loss in the on-state to the modal propagation loss in the off-state. FOM_{modal} is a direct measure of the ER to the IL.

$$\text{FOM}_{modal} = \frac{\text{propagation loss}_{on-state}}{\text{propagation loss}_{off-state}} \tag{6-1}$$

To optimize h_2 and w, h_1 is set to be 100 nm and the thickness of the VO_2 layer is set to be 30 nm. Figure 6.4 illustrates the FOM_{modal} as a function of w for different values of h_2.

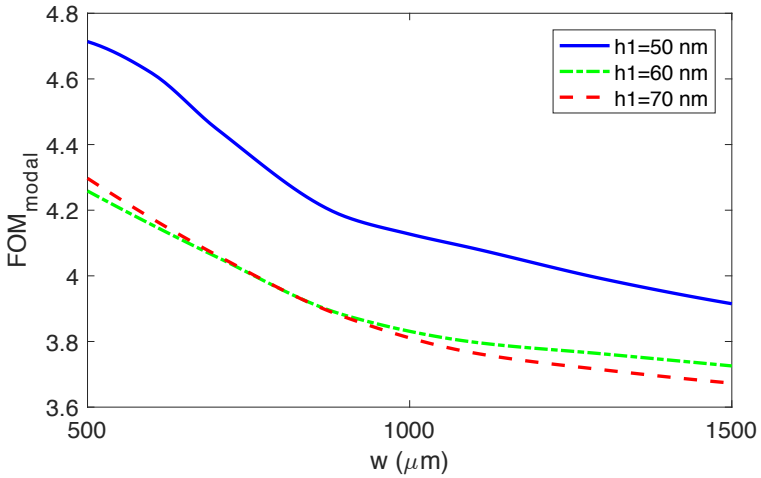

Figure 6.4 - FOMmodal versus the width of the Si-rib waveguide for different values for h1.

The highest FOM_{modal} is achieved at h_2= 50 nm and w = 500 nm. The mode vanishes when reducing h_2 less than 50 nm as well reducing w less than 500 nm. Figure 6.5 shows the FOM_{modal} versus the thickness of the VO_2 layer at h_2= 50 nm and w = 500 nm.

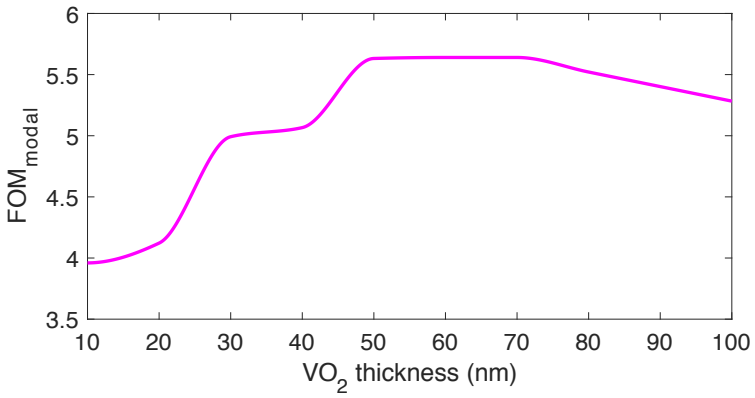

Figure 6.5 - FOM_{modal} versus the thickness of the VO2 layer at h2= 50 nm and w = 500 nm.

The insertion loss and extinction ratio increases as the thickness of the VO_2 layer increases; however, the FOM_{modal} reaches its maximum value over the range from 50 to 70 nm of thickness of VO_2 layer. After 70 nm thickness the insertion loss rises rapidly reducing the FOM_{modal}. The thickness of the VO_2 layer is selected to be 50 nm, because the thinner the VO_2 layer, the less voltage needed to make the transition from the dielectric state to the metallic state.

6.1.5 Modulation properties of the hybrid electro-optical switch

Finite difference time domain simulations, with perfect matching layer (PML) absorbing boundary conditions, were conducted to simulate and analyze this design. Figure 6.6 shows the normalized mode intensity, with respect to the input intensity, at the center of the Si layer along the propagation length, for 1-μm long modulation section, when there is no external electric field and with applied external electric field across the modulation section.

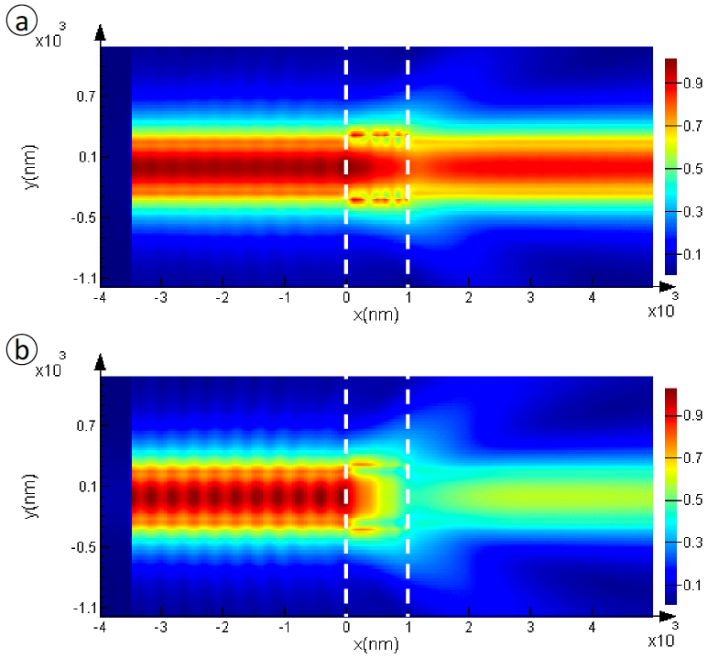

Figure 6.6 - The normalized intensity, with respect to the input, of the guided mode at the center of the Si layer for (a) off and (b) on-states. The dashed lines indicate the modulation section.

Figure 6.7 shows the IL and ER versus wavelength for 1 μm long modulation section at the telecommunication wavelength (1.55 μm). An IL of 0.97 dB and ER of 4.85 dB are achieved for 1-μm long modulation section, at the telecommunications wavelength (1.55 μm). Both the IL and ER are almost constant over a wide range of bandwidth.

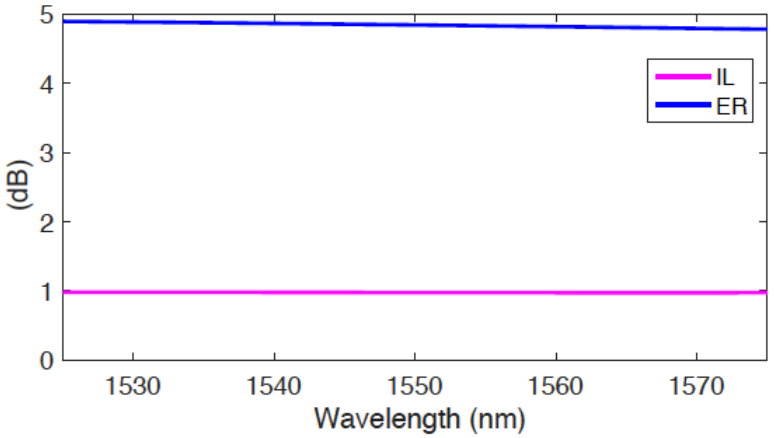

Figure 6.7 - IL and ER as a function of wavelength for 1-μm long modulation section.

Increasing the length of the modulation section increases the IL and the ER as illustrated in Figure 6.8. It is clear from the Figure 6.8 that the relation between the the

length of the modulation section and both the IL and the ER is linear. As illustrated, the proposed electro-optical switch has an IL per unit length of 0.88 dB/μm; as well as, an ER per unit length of 4.32 dB/μm. FOM is defined as the ratio between the ER and IL. For the proposed design, the FOM is almost constant, with value of 4.9, for different lengths of the modulation section.

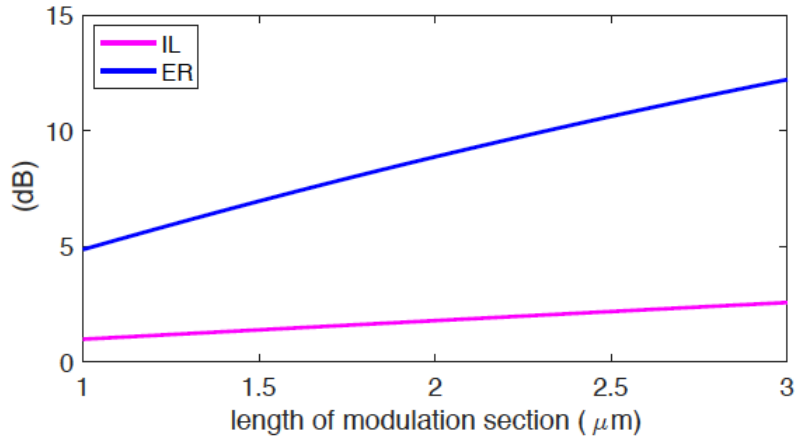

Figure 6.8 - IL and ER, at 1.55 μm, versus the length of modulation section.

The phase transition from dielectric state to conducting state of VO_2 can be produced by applying external electric field to the Ag contacts within nanosecond time scales [143], [144]. However, the modulation speed of the devices is limited by the relaxation time VO_2 needs to restore its dielectric state [145]. The modulation speed of the proposed design is estimated to be 1 GHz based on experimental measurements of electro-optical modulators based on VO_2 [144]. This limiting factor can be improved by integrating an electrical biasing to quickly root out excess carriers; this technique is used in carrier depletion type Si-optical modulators [37].

Around room temperature, VO_2 exhibits an electric field threshold of 6.5×10^7 V/m [132]. The thickness of VO_2 layer in the proposed design is 50 nm. Thus the required drive voltage of the proposed electro-optical switch is 3.25 V.

6.1.6 Conclusion

An electro-optic hybrid plasmonic switch based on the phase change properties of VO_2 is developed and verified numerically using FDTD simulations. We demonstrated a 4.32 dB/μm ER per unit length and 0.88 dB/μm IL per unit length. The drive voltage calculated to be around 3.3 V. the proposed electro-optic switch exhibits a wide

bandwidth operation near the telecommunication wavelength. The design has advantages including, but not limited to, small device foot-print and compatibility to be integrated on-chip. Such hybrid plasmonic electro-optic switch based modulators, with high extinction ratios, insertion losses, and small foot-print are the milestone for integrating photonic circuitries to the existing electronic circuitries.

Chapter 7 Conclusions and future work

Optical technology is revolutionizing both optical communication systems and on-chip interconnects. Electro-optical modulators are key components in optical communication systems since they modulate digital electronic signals to optical signals to travel over the optical fibers for long distances with minor losses. Also, electro-optical modulators that can be integrated on the same substrate with electronic circuits offering solution to the bottleneck of on-chip copper interconnects.

The same time the demand for optical interconnects increased, a remarkable expansion happened to the silicon photonics. The same material used for building electronic chips for decades is, now, mature enough to build optical integrated chips. Nowadays, integrated optoelectronics, integrated monolithically in Si, combine both the performance of photonics and the intelligence of electronics.

Many Si EOMs are designed and studied utilizing carrier concentration change effect, the most important modulation mechanism affecting the real and imaginary parts of the refractive index of Si. This mechanism has a drawback that the life time of carriers limits the speed of the devices. This raised the necessity for investigating hybrid combinations of novel materials with silicon. This fulfils the functions silicon is incapable to provide alone. Organic polymers, indium-tin-oxide, and vanadium dioxide are among these novel materials.

In this thesis, a brief background about the mechanisms, materials, and structures used for external optical modulation are presented. Also, state-of-art EOMs are introduced. After this, novel electro-optical modulators, based on different active material and structures, are proposed and studied.

An organic hybrid-plasmonic optical directional coupler is studied utilizing the change of polymer electro-optic characteristics upon applying an external electric field. A finite element method used to simulate and study this design. For 39 μm modulation length, an extinction ratio of 14.34 dB is achieved.

A low insertion loss compact silicon electro-optic modulator is studied, using a finite difference time domain method with perfect matching layer (PML) absorbing boundary conditions. The EOM is based on tri-coupled waveguides, two silicon slot waveguides separated by an ITO based plasmonic waveguide. The electrical tuning mechanism is designed to both change the coupling conditions and introduce additional

intrinsic losses upon applying an external electric field to the middle ITO based plasmonic waveguide. Based on this design, extinction ratio of 6.14dB and insertion losses of 0.06 dB are realized at 21 μm modulator length; as well as, extinction ratio of 11.43 dB and insertion losses of 1.65 dB are realized at 34 μm modulator length.

A hybrid silicon electro-absorption modulator is introduced and analyzed. The device is based on dielectric slot waveguide with an ITO plasmonic modulation section. For 10 μm long modulation section, an extinction ratio of 15.49 dB and an insertion loss of 1.01 dB are achieved. Modal and finite difference time domain analysis were performed to verify and simulate the design.

Optical switch based on a hybrid plasmonic-vanadium dioxide waveguide is presented. The power-attenuating mechanism takes the advantage of the phase change properties of vanadium dioxide that exhibits a change in the real and complex refractive indices upon switching from the dielectric phase to the metallic phase. Under the telecommunication wavelength, an ER per unit length of 4.32 dB/μm and IL per unit length of 0.88 dB/μm are realized. Finite difference time domain analysis used simulate and study the design.

Different materials used for different device structures. Electro-optical polymers utilize linear Pockels effect with an electro-optic coefficient that is higher five times than lithium niobate. EOPs can be used in structures based on interference such as directional couplers and Mach-Zehnder interferometers. Electro-optical polymers based modulators have very low insertion loss. However, they have large device footprints since the modulation mechanism is based on changing the phase of the propagating waves. Also, devices based on EOPs are easier to fabricate compared with devices based on other active materials.

Carrier density of ITO can be controlled when used in MOS-structures. ITO exhibits epsilon-near-zero effect. This effect is appealing for researches to tune the real and imaginary parts of the permittivity of the ITO. Devices based on indium-tin-oxide have high extinction ratios and small device footprints. Yet, they suffer from high insertion losses due to the strong field enhancement in the lossy plasmonic waveguides. These devices have a very high speeds.

Vanadium dioxide is considered as a phase change material. It undergoes a transformation from semiconductor state to metallic state when subjected to external

stimulus. It can be used for electro-optic modulation. Devices based on VO_2 have small footprints and high extinction ratios. Still, the modulation speed of such devices is estimated to be 1 GHz, based on experimental measurements, due to the relaxation time VO_2 needs to restore its dielectric state. As extension to this work, a Si race-track resonator based modulator is to be studied featuring VO_2 deposited on one of the straight sides of the race-track resonator.

Fabricating these designs and to experimentally measuring all the parameters are planned as an extension to this work. Also, combining more than one active material in the same design is to be studied.

The proposed electro-optical devices have the advantages of small device foot-print and compatibility with the existing VLSI-CMOS technology. Also, broadband operation of these modulators are promising due to the nonexistence of resonance effect. Such silicon-on insulator electro-optical modulators with high extinction ratios, low insertion losses, and low power consumptions are fundamental for bridging photonic platforms to the existing electronics. A new stages of integration will ultimately set.

References

[1] “Fiber Optic Technology and its role in the Information Revolution.” [Online]. Available: https://www.ece.umd.edu/~davis/optfib.html. [Accessed: 27-Feb-2018].

[2] “Smoke Signals,” *The History of Media (The Beginning-1950 A.D.)*. [Online]. Available: http://thehistoryofmedia.weebly.com/smoke-signals.html. [Accessed: 27-Feb-2018].

[3] J. Hecht, “Guiding Light and Luminous Fountains,” in *City of Light: The Story of Fiber Optics*, Oxford University Press, 2004, pp. 12–27.

[4] J. Tyndall, *Notes of a course of nine lectures on light delivered at the Royal institution of Great Britain April 8-June 3, 1869*. London, Longmans, 1870.

[5] “How does fiber optics work?,” *Explain that Stuff*. [Online]. Available: http://www.explainthatstuff.com/fiberoptics.html. [Accessed: 27-Feb-2018].

[6] A. Chen and E. Murphy, *Broadband Optical Modulators: Science, Technology, and Applications - CRC Press Book*. 2011.

[7] Cisco, “Cisco Global Cloud Index: Forecast and Methodology, 2016–2021 White Paper,” *Cisco*. [Online]. Available: https://www.cisco.com/c/en/us/solutions/collateral/service-provider/global-cloud-index-gci/white-paper-c11-738085.html. [Accessed: 28-Feb-2018].

[8] C. Peucheret and D. Fotonik, “Direct & External Modulation Direct and External Modulation of Light,” Feb. 2018.

[9] S. Laval, L. Vivien, E. Cassan, D. Marris-Morini, and J.-M. Fédéli, “New Interconnect Schemes,” in *Electronic Devices Architectures for the NANO-CMOS Era*, 0 vols., Pan Stanford Publishing, 2008, pp. 159–183.

[10] D. A. B. Miller, “Optical interconnects to silicon,” *IEEE J. Sel. Top. Quantum Electron.*, vol. 6, no. 6, pp. 1312–1317, Nov. 2000.

[11] A. Benner, “Optical interconnect opportunities in supercomputers and high end computing,” in *OFC/NFOEC*, 2012, pp. 1–60.

[12] S. Libertino and A. Sciuto, “Electro-Optical Modulators in Silicon,” in *Optical Interconnects*, Springer, Berlin, Heidelberg, 2006, pp. 53–95.

[13] L. Liao *et al.*, “High speed silicon Mach-Zehnder modulator,” *Opt. Express*, vol. 13, no. 8, pp. 3129–3135, Apr. 2005.

[14] W. M. J. Green, M. J. Rooks, L. Sekaric, and Y. A. Vlasov, “Ultra-compact, low RF power, 10 Gb/s silicon Mach-Zehnder modulator,” *Opt. Express*, vol. 15, no. 25, pp. 17106–17113, Dec. 2007.

[15] P. Dong *et al.*, “Wavelength-tunable silicon microring modulator,” *Opt. Express*, vol. 18, no. 11, pp. 10941–10946, May 2010.

[16] A. Liu *et al.*, “A high-speed silicon optical modulator based on a metal–oxide–semiconductor capacitor,” *Nature*, vol. 427, no. 6975, pp. 615–618, Feb. 2004.

[17] F. Y. Gardes, D. J. Thomson, N. G. Emerson, and G. T. Reed, “40 Gb/s silicon photonics modulator for TE and TM polarisations,” *Opt. Express*, vol. 19, no. 12, pp. 11804–11814, Jun. 2011.

[18] L. Liao *et al.*, “Phase modulation efficiency and transmission loss of silicon optical phase shifters,” *IEEE J. Quantum Electron.*, vol. 41, no. 2, pp. 250–257, Feb. 2005.

[19] R. Soref and B. Bennett, “Electrooptical effects in silicon,” *IEEE J. Quantum Electron.*, vol. 23, no. 1, pp. 123–129, Jan. 1987.

[20] G. T. Reed, G. Mashanovich, F. Y. Gardes, and D. J. Thomson, “Silicon optical modulators,” *Nat. Photonics*, vol. 4, no. 8, pp. 518–526, Aug. 2010.
[21] M. R. Watts, D. C. Trotter, R. W. Young, and A. L. Lentine, “Ultralow power silicon microdisk modulators and switches,” in *2008 5th IEEE International Conference on Group IV Photonics*, 2008, pp. 4–6.
[22] M. R. Watts, W. A. Zortman, D. C. Trotter, R. W. Young, and A. L. Lentine, “Vertical junction silicon microdisk modulators and switches,” *Opt. Express*, vol. 19, no. 22, pp. 21989–22003, Oct. 2011.
[23] J. C. Rosenberg *et al.*, “A 25 Gbps silicon microring modulator based on an interleaved junction,” *Opt. Express*, vol. 20, no. 24, pp. 26411–26423, Nov. 2012.
[24] V. J. Sorger, N. D. Lanzillotti-Kimura, R.-M. Ma, and X. Zhang, “Ultra-compact silicon nanophotonic modulator with broadband response,” *Nanophotonics*, vol. 1, pp. 17–22, Jul. 2012.
[25] “Silicon Photonics Design by Lukas Chrostowski,” *Cambridge Core*. [Online]. Available: /core/books/silicon-photonics-design/BF3CF13E8542BCE67FD2BBC7104ECEAB. [Accessed: 12-Sep-2017].
[26] M. J. Deen and P. K. Basu, *Silicon Photonics: Fundamentals and Devices*. Chichester, UK: John Wiley & Sons, Ltd, 2012.
[27] Q. Xu, B. Schmidt, S. Pradhan, and M. Lipson, “Micrometre-scale silicon electro-optic modulator,” *Nature*, vol. 435, no. 7040, pp. 325–327, May 2005.
[28] Q. Xu, S. Manipatruni, B. Schmidt, J. Shakya, and M. Lipson, “12.5 Gbit/s silicon micro-ring silicon modulators,” in *2007 Conference on Lasers and Electro-Optics (CLEO)*, 2007, pp. 1–2.
[29] P. Dong, L. Chen, and Y. Chen, “High-speed low-voltage single-drive push-pull silicon Mach-Zehnder modulators,” *Opt. Express*, vol. 20, no. 6, pp. 6163–6169, Mar. 2012.
[30] C. Ye, S. Khan, Z. R. Li, E. Simsek, and V. J. Sorger, “#x03BB;-Size ITO and Graphene-Based Electro-Optic Modulators on SOI,” *IEEE J. Sel. Top. Quantum Electron.*, vol. 20, no. 4, pp. 40–49, Jul. 2014.
[31] M. Liu *et al.*, “A graphene-based broadband optical modulator,” *Nature*, vol. 474, no. 7349, pp. 64–67, Jun. 2011.
[32] J. T. Kim, “CMOS-compatible hybrid plasmonic modulator based on vanadium dioxide insulator-metal phase transition,” *Opt. Lett.*, vol. 39, no. 13, pp. 3997–4000, Jul. 2014.
[33] F. Yi, E. Shim, A. Y. Zhu, H. Zhu, J. C. Reed, and E. Cubukcu, “Voltage tuning of plasmonic absorbers by indium tin oxide,” *Appl. Phys. Lett.*, vol. 102, no. 22, p. 221102, 2013.
[34] V. E. Babicheva *et al.*, “Towards CMOS-compatible nanophotonics: Ultra-compact modulators using alternative plasmonic materials,” *Opt. Express*, vol. 21, no. 22, pp. 27326–27337, Nov. 2013.
[35] Y. Kim, M. Takenaka, T. Osada, M. Hata, and S. Takagi, “Strain-induced enhancement of plasma dispersion effect and free-carrier absorption in SiGe optical modulators,” *Sci. Rep.*, vol. 4, p. srep04683, Apr. 2014.
[36] N. A. Wasley, *Nano-photonics in III-V Semiconductors for Integrated Quantum Optical Circuits*. Cham: Springer International Publishing, 2014.
[37] A. Liu *et al.*, “High-speed optical modulation based on carrier depletion in a silicon waveguide,” *Opt. Express*, vol. 15, no. 2, pp. 660–668, Jan. 2007.

[38] M. Brongersma, “Introductory lecture: Nanoplasmonics,” *Faraday Discuss*, vol. 178, May 2015.
[39] M. L. Brongersma and V. M. Shalaev, “Applied physics. The case for plasmonics,” *Science*, vol. 328, no. 5977, pp. 440–441, Apr. 2010.
[40] J. T. Kim, “Silicon Optical Modulators Based on Tunable Plasmonic Directional Couplers,” *IEEE J. Sel. Top. Quantum Electron.*, vol. 21, no. 4, pp. 184–191, Jul. 2015.
[41] J. Kim, J. Koo, and J. H. Lee, “All-fiber acousto-optic modulator based on a cladding-etched optical fiber for active mode-locking,” *Photonics Res.*, vol. 5, no. 5, pp. 391–395, Oct. 2017.
[42] G. Cocorullo, F. G. Della Corte, and I. Rendina, “Temperature dependence of the thermo-optic coefficient in crystalline silicon between room temperature and 550 K at the wavelength of 1523 nm,” *Appl. Phys. Lett.*, vol. 74, no. 22, pp. 3338–3340, May 1999.
[43] M. Bertolotti *et al.*, “Temperature dependence of the refractive index in semiconductors,” *JOSA B*, vol. 7, no. 6, pp. 918–922, Jun. 1990.
[44] C. Ironside, “Linear electro-optic effect, electroabsorption and electrorefraction,” IOP Publishing, 2017, p. .
[45] P. YU and M. Cardona, “Optical Properties I,” in *Fundamentals of Semiconductors: Physics and Materials Properties*, 4th ed., Berlin Heidelberg: Springer-Verlag, 2010, pp. 243–344.
[46] N. W. Ashcroft and N. D. Mermin, *Solid State Physics*, 1 edition. New York: Brooks Cole, 1976.
[47] C.-T. Zheng, C.-S. Ma, X. Yan, X.-Y. Wang, and D.-M. Zhang, “Design of a polymer directional coupler electro-optic switch using two-section reversed electrodes,” *Appl. Phys. B*, vol. 96, no. 1, pp. 95–103, May 2009.
[48] E. L. Wooten *et al.*, “A Review of Lithium Niobate Modulators for Fiber-Optic Communications Systems,” *Sel. Top. Quantum Electron. IEEE J. Of*, vol. 6, pp. 69–82, Feb. 2000.
[49] J. Nayyer and H. Nagata, “Suppression of thermal drifts of high speed Ti:LiNbO/sub 3/ optical modulators,” *IEEE Photonics Technol. Lett.*, vol. 6, no. 8, pp. 952–955, Aug. 1994.
[50] J. Tang, S. Yang, and A. Bhatranand, “Electro-Optic Barium Titanate Waveguide Modulators with Transparent Conducting Oxide Electrodes,” in *Conference on Lasers and Electro-Optics/Pacific Rim 2009 (2009), paper TUP6_2*, 2009, p. TUP6_2.
[51] H. M. K. Wong and A. S. Helmy, “Performance Enhancement of Nanoscale VO2 Modulators Using Hybrid Plasmonics,” *J. Light. Technol.*, vol. 36, no. 3, pp. 797–808, Feb. 2018.
[52] A. Joushaghani, B. A. Kruger, S. Paradis, D. Alain, J. Stewart Aitchison, and J. K. S. Poon, “Sub-volt broadband hybrid plasmonic-vanadium dioxide switches,” *Appl. Phys. Lett.*, vol. 102, no. 6, p. 061101, Feb. 2013.
[53] † Tae-Dong Kim *et al.*, “Ultralarge and Thermally Stable Electro-Optic Activities from Supramolecular Self-Assembled Molecular Glasses,” 03-Jan-2007. [Online]. Available: http://pubs.acs.org/doi/abs/10.1021/ja067970s. [Accessed: 11-Aug-2016].
[54] D. Jin *et al.*, “EO polymer modulators reliability study,” in *Organic Photonic Materials and Devices XII*, 2010, vol. 7599, p. 75990H.

[55] B. Li *et al.*, “Recent advances in commercial electro-optic polymer modulator,” in *2007 Asia Optical Fiber Communication and Optoelectronics Conference*, 2007, pp. 115–117.
[56] P. P. Edwards, A. Porch, M. O. Jones, D. V. Morgan, and R. M. Perks, “Basic materials physics of transparent conducting oxides,” *Dalton Trans. Camb. Engl. 2003*, no. 19, pp. 2995–3002, Oct. 2004.
[57] P. West, S. Ishii, G. Naik, N. Emani, V. M. Shalaev, and A. Boltasseva, “Searching for Better Plasmonic Materials,” *ArXiv09112737 Phys.*, Nov. 2009.
[58] E. Feigenbaum, K. Diest, and H. A. Atwater, “Unity-Order Index Change in Transparent Conducting Oxides at Visible Frequencies,” *Nano Lett.*, vol. 10, no. 6, pp. 2111–2116, Jun. 2010.
[59] “The increasing importance of extinction ratio in telecommunications.” [Online]. Available: http://www.lightwaveonline.com/articles/2005/09/the-increasing-importance-of-extinction-ratio-in-telecommunications-53915762.html. [Accessed: 07-Mar-2018].
[60] R. Hunsperger, *Integrated Optics: Theory and Technology*, 5th ed. Berlin Heidelberg: Springer-Verlag, 2002.
[61] Z. Lu, W. Zhao, and K. Shi, “Ultracompact Electroabsorption Modulators Based on Tunable Epsilon-Near-Zero-Slot Waveguides,” *IEEE Photonics J.*, vol. 4, no. 3, pp. 735–740, Jun. 2012.
[62] M. Y. Abdelatty, A. O. Zaki, and M. A. Swillam, “Hybrid silicon plasmonic organic directional coupler-based modulator,” *Appl. Phys. A*, vol. 123, no. 1, p. 11, Jan. 2017.
[63] J. A. Dionne, K. Diest, L. A. Sweatlock, and H. A. Atwater, “PlasMOStor: A Metal−Oxide−Si Field Effect Plasmonic Modulator,” 26-Jan-2009. [Online]. Available: http://pubs.acs.org/doi/abs/10.1021/nl803868k?journalCode=nalefd. [Accessed: 11-Aug-2016].
[64] S. Zhu, G. Q. Lo, and D. L. Kwong, “Electro-absorption modulation in horizontal metal-insulator-silicon-insulator-metal nanoplasmonic slot waveguides,” *Appl. Phys. Lett.*, vol. 99, no. 15, p. 151114, Oct. 2011.
[65] B. Janjan, A. Zarifkar, and M. Miri, “Ultra-Compact High-Speed Electro-Optical Modulator with Extremely Low Energy Consumption Based on Polymer-Filled Hybrid Plasmonic Waveguide,” *Plasmonics*, vol. 11, no. 2, pp. 509–514, Apr. 2016.
[66] X. Sun, L. Zhou, H. Zhu, Q. Wu, X. Li, and J. Chen, “Design and Analysis of a Miniature Intensity Modulator Based on a Silicon-Polymer-Metal Hybrid Plasmonic Waveguide,” *IEEE Photonics J.*, vol. 6, no. 3, pp. 1–10, Jun. 2014.
[67] A. O. Zaki, K. Kirah, and M. A. Swillam, “Hybrid plasmonic electro-optical modulator,” *Appl. Phys. A*, vol. 122, no. 4, p. 473, Apr. 2016.
[68] D. C. Zografopoulos, M. A. Swillam, L. A. Shahada, and R. Beccherelli, “Hybrid electro-optic plasmonic modulators based on directional coupler switches,” *Appl. Phys. A*, vol. 122, no. 4, pp. 1–6, Mar. 2016.
[69] L. Jin, Q. Chen, W. Liu, and S. Song, “Electro-absorption Modulator with Dual Carrier Accumulation Layers Based on Epsilon-Near-Zero ITO,” *Plasmonics*, vol. 11, no. 4, pp. 1087–1092, Aug. 2016.
[70] A. P. Vasudev, J.-H. Kang, J. Park, X. Liu, and M. L. Brongersma, “Electro-optical modulation of a silicon waveguide with an ‘epsilon-near-zero’ material,” *Opt. Express*, vol. 21, no. 22, pp. 26387–26397, Nov. 2013.

[71] K. Shi and Z. Lu, “Field-effect optical modulation based on epsilon-near-zero conductive oxide,” *Opt. Commun.*, vol. 370, no. Supplement C, pp. 22–28, Jul. 2016.
[72] J. Baek, J.-B. You, and K. Yu, “Free-carrier electro-refraction modulation based on a silicon slot waveguide with ITO,” *Opt. Express*, vol. 23, no. 12, pp. 15863–15876, Jun. 2015.
[73] J.-S. Kim and J. T. Kim, “Silicon electro-optic modulator based on an ITO-integrated tunable directional coupler,” *J. Phys. Appl. Phys.*, vol. 49, no. 7, p. 075101, 2016.
[74] H. Zhao, Y. Wang, A. Capretti, L. D. Negro, and J. Klamkin, “Broadband Electroabsorption Modulators Design Based on Epsilon-Near-Zero Indium Tin Oxide,” *IEEE J. Sel. Top. Quantum Electron.*, vol. 21, no. 4, pp. 192–198, Jul. 2015.
[75] H. W. Lee *et al.*, “Nanoscale Conducting Oxide PlasMOStor,” *Nano Lett.*, vol. 14, no. 11, pp. 6463–6468, Nov. 2014.
[76] R. M. Briggs, I. M. Pryce, and H. A. Atwater, “Compact silicon photonic waveguide modulator based on the vanadium dioxide metal-insulator phase transition,” *Opt. Express*, vol. 18, no. 11, pp. 11192–11201, May 2010.
[77] J. D. Ryckman, K. A. Hallman, R. E. Marvel, R. F. Haglund, and S. M. Weiss, “Ultra-compact silicon photonic devices reconfigured by an optically induced semiconductor-to-metal transition,” *Opt. Express*, vol. 21, no. 9, pp. 10753–10763, May 2013.
[78] J. T. Kim, “CMOS-compatible hybrid plasmonic modulator based on vanadium dioxide insulator-metal phase transition,” *Opt. Lett.*, vol. 39, no. 13, pp. 3997–4000, Jul. 2014.
[79] M. Sun, W. Shieh, and R. R. Unnithan, “Design of plasmonic modulators with vanadium dioxide on silicon-on-insulator,” in *2017 IEEE Photonics Conference (IPC)*, 2017, pp. 77–85.
[80] P. Markov, K. Appavoo, R. F. Haglund, and S. M. Weiss, “Hybrid Si-VO_2-Au optical modulator based on near-field plasmonic coupling,” *Opt. Express*, vol. 23, no. 5, pp. 6878–6887, Mar. 2015.
[81] A. Joushaghani, B. A. Kruger, S. Paradis, D. Alain, J. Stewart Aitchison, and J. K. S. Poon, “Sub-volt broadband hybrid plasmonic-vanadium dioxide switches,” *Appl. Phys. Lett.*, vol. 102, no. 6, p. 061101, Feb. 2013.
[82] H. M. K. Wong and A. S. Helmy, “Performance Enhancement of Nanoscale VO2 Modulators Using Hybrid Plasmonics,” *J. Light. Technol.*, vol. 36, no. 3, pp. 797–808, Feb. 2018.
[83] D. C. Zografopoulos, M. A. Swillam, L. A. Shahada, and R. Beccherelli, “Hybrid electro-optic plasmonic modulators based on directional coupler switches,” *Appl. Phys. A*, vol. 122, no. 4, p. 344, Apr. 2016.
[84] T. Baba *et al.*, “50-Gb/s ring-resonator-based silicon modulator,” *Opt. Express*, vol. 21, no. 10, pp. 11869–11876, May 2013.
[85] G. Li *et al.*, “25Gb/s 1V-driving CMOS ring modulator with integrated thermal tuning,” *Opt. Express*, vol. 19, no. 21, pp. 20435–20443, Oct. 2011.
[86] A. Liu *et al.*, “A high-speed silicon optical modulator based on a metal–oxide–semiconductor capacitor,” *Nature*, vol. 427, no. 6975, pp. 615–618, Feb. 2004.
[87] H. Zhao, X. G. Guang, and J. Huang, “Novel optical directional coupler based on surface plasmon polaritons,” *Phys. E Low-Dimens. Syst. Nanostructures*, vol. 40, no. 10, pp. 3025–3029, Sep. 2008.

[88] A. Krasavin and A. Zayats, “Photonic Signal Processing on Electronic Scales: Electro-Optical Field-Effect Nanoplasmonic Modulator,” *Phys. Rev. Lett.*, vol. 109, no. 5, Jul. 2012.
[89] C.-H. Du and Y.-P. Chiou, “Vertical Directional Couplers With Ultra-Short Coupling Length Based on Hybrid Plasmonic Waveguides,” *J. Light. Technol.*, vol. 32, no. 11, pp. 2065–2071, Jun. 2014.
[90] J. Luo *et al.*, “Facile synthesis of highly efficient phenyltetraene-based nonlinear optical chromophores for electrooptics,” *Org. Lett.*, vol. 8, no. 7, pp. 1387–1390, Mar. 2006.
[91] T.-D. Kim *et al.*, “Ultralarge and thermally stable electro-optic activities from supramolecular self-assembled molecular glasses,” *J. Am. Chem. Soc.*, vol. 129, no. 3, pp. 488–489, Jan. 2007.
[92] M. Lee *et al.*, “Broadband Modulation of Light by Using an Electro-Optic Polymer,” *Science*, vol. 298, no. 5597, pp. 1401–1403, Nov. 2002.
[93] J.-M. Brosi, C. Koos, L. C. Andreani, M. Waldow, J. Leuthold, and W. Freude, “High-speed low-voltage electro-optic modulator with a polymer-infiltrated silicon photonic crystal waveguide,” *Opt. Express*, vol. 16, no. 6, pp. 4177–4191, Mar. 2008.
[94] C.-T. Zheng, C.-S. Ma, X. Yan, X.-Y. Wang, and D.-M. Zhang, “Analysis of response characteristics for polymer directional coupler electro-optic switches,” *Opt. Commun.*, vol. 281, no. 24, pp. 5998–6005, Dec. 2008.
[95] R. S. Jacobsen *et al.*, “Strained silicon as a new electro-optic material,” *Nature*, vol. 441, no. 7090, pp. 199–202, May 2006.
[96] J. Luo, T.-D. Kim, and A. K.-Y. Jen, “Unprecedented Electro-optic Properties in Polymers and Dendrimers Enabled by Click Chemistry Based on the Diels–Alder Reactions,” in *Click Chemistry for Biotechnology and Materials Science*, John Wiley & Sons, Ltd, 2009, pp. 379–398.
[97] B. Tatian, “Fitting refractive-index data with the Sellmeier dispersion formula,” *Appl. Opt.*, vol. 23, no. 24, pp. 4477–4485, Dec. 1984.
[98] Y. Song, J. Wang, Q. Li, M. Yan, and M. Qiu, “Broadband coupler between silicon waveguide and hybrid plasmonic waveguide,” *Opt. Express*, vol. 18, no. 12, pp. 13173–13179, Jun. 2010.
[99] C. Lin and A. S. Helmy, “Dynamically reconfigurable nanoscale modulators utilizing coupled hybrid plasmonics,” *Sci. Rep.*, vol. 5, p. srep12313, Jul. 2015.
[100] A. O. Zaki, K. Kirah, and M. A. Swillam, “Hybrid plasmonic electro-optical modulator,” *Appl. Phys. A*, vol. 122, no. 4, p. 473, Apr. 2016.
[101] A. Chen and E. Murphy, Eds., *Broadband Optical Modulators: Science, Technology, and Applications*, 1 edition. Boca Raton, 2011.
[102] G. Sinatkas, A. Pitilakis, D. C. Zografopoulos, R. Beccherelli, and E. E. Kriezis, “Transparent conducting oxide electro-optic modulators on silicon platforms: A comprehensive study based on the drift-diffusion semiconductor model,” *J. Appl. Phys.*, vol. 121, no. 2, p. 023109, Jan. 2017.
[103] T. Baehr-Jones *et al.*, “Nonlinear polymer-clad silicon slot waveguide modulator with a half wave voltage of 0.25V,” *Appl. Phys. Lett.*, vol. 92, no. 16, p. 163303, Apr. 2008.
[104] Y. F. Ma and D. W. Huang, “A compact slot waveguide directional coupler-based silicon-on-insulator polarization splitter,” in *2008 5th IEEE International Conference on Group IV Photonics*, 2008, pp. 297–298.

[105] "FDTD Solutions | Lumerical's Nanophotonic FDTD Simulation Software." [Online]. Available: https://www.lumerical.com/tcad-products/fdtd/. [Accessed: 21-Dec-2016].
[106] M. K. Emsley, O. Dosunmu, and M. S. Unlu, "High-speed resonant-cavity-enhanced silicon photodetectors on reflecting silicon-on-insulator substrates," *IEEE Photonics Technol. Lett.*, vol. 14, no. 4, pp. 519–521, Apr. 2002.
[107] "MODE Solutions | Waveguide Mode Solver and Propagation Simulator." [Online]. Available: https://www.lumerical.com/tcad-products/mode/. [Accessed: 27-Jul-2016].
[108] D. F. Edwards, "Silicon (Si)*," in *Handbook of Optical Constants of Solids*, E. D. Palik, Ed. Burlington: Academic Press, 1997, pp. 547–569.
[109] H. R. Philipp, "Silicon Dioxide (SiO2) (Glass) A2 - Palik, Edward D.," in *Handbook of Optical Constants of Solids*, Burlington: Academic Press, 1997, pp. 749–763.
[110] P. B. Johnson and R. W. Christy, "Optical Constants of the Noble Metals," *Phys. Rev. B*, vol. 6, no. 12, pp. 4370–4379, Dec. 1972.
[111] D. L. Wood, K. Nassau, T. Y. Kometani, and D. L. Nash, "Optical properties of cubic hafnia stabilized with yttria," *Appl. Opt.*, vol. 29, no. 4, pp. 604–607, Feb. 1990.
[112] "FDTD Solutions | Lumerical's Nanophotonic FDTD Simulation Software." [Online]. Available: https://www.lumerical.com/tcad-products/fdtd/.
[113] "COMSOL Multiphysics® Modeling Software." [Online]. Available: https://www.comsol.es/.
[114] D. A. B. Miller, "Device Requirements for Optical Interconnects to Silicon Chips," *Proc. IEEE*, vol. 97, no. 7, pp. 1166–1185, Jul. 2009.
[115] M. Kauranen and A. V. Zayats, "Nonlinear plasmonics," *Nat. Photonics*, vol. 6, no. 11, p. nphoton.2012.244, Nov. 2012.
[116] M. Streshinsky *et al.*, "Low power 50 Gb/s silicon traveling wave Mach-Zehnder modulator near 1300 nm," *Opt. Express*, vol. 21, no. 25, pp. 30350–30357, Dec. 2013.
[117] U. Koch, C. Hoessbacher, J. Niegemann, C. Hafner, and J. Leuthold, "Digital Plasmonic Absorption Modulator Exploiting Epsilon-Near-Zero in Transparent Conducting Oxides," *IEEE Photonics J.*, vol. 8, pp. 1–1, Feb. 2016.
[118] C. Ye, S. Khan, Z. R. Li, E. Simsek, and V. J. Sorger, "#x03BB;-Size ITO and Graphene-Based Electro-Optic Modulators on SOI," *IEEE J. Sel. Top. Quantum Electron.*, vol. 20, no. 4, pp. 40–49, Jul. 2014.
[119] V. E. Babicheva, A. Boltasseva, and A. V. Lavrinenko, "Transparent conducting oxides for electro-optical plasmonic modulators," *Nanophotonics*, vol. 4, no. 1, pp. 165–185, 2015.
[120] G. T. Reed and C. E. Jason Png, "Silicon optical modulators," *Mater. Today*, vol. 8, no. 1, pp. 40–50, Jan. 2005.
[121] A. Liu *et al.*, "A high-speed silicon optical modulator based on a metal–oxide–semiconductor capacitor," *Nature*, vol. 427, no. 6975, pp. 615–618, Feb. 2004.
[122] Q. Xu, B. Schmidt, S. Pradhan, and M. Lipson, "Micrometre-scale silicon electro-optic modulator," *Nature*, vol. 435, no. 7040, pp. 325–327, May 2005.
[123] R. Soref and B. Bennett, "Electrooptical effects in silicon," *IEEE J. Quantum Electron.*, vol. 23, no. 1, pp. 123–129, Jan. 1987.

[124] P. Markov, K. Appavoo, R. F. Haglund, and S. M. Weiss, “Hybrid Si-VO_2-Au optical modulator based on near-field plasmonic coupling,” *Opt. Express*, vol. 23, no. 5, pp. 6878–6887, Mar. 2015.
[125] E. L. Wooten *et al.*, “A review of lithium niobate modulators for fiber-optic communications systems,” *IEEE J. Sel. Top. Quantum Electron.*, vol. 6, no. 1, pp. 69–82, Jan. 2000.
[126] M. Hochberg *et al.*, “Terahertz all-optical modulation in a silicon–polymer hybrid system,” *Nat. Mater.*, vol. 5, no. 9, pp. 703–709, Sep. 2006.
[127] L. Alloatti *et al.*, “42.7 Gbit/s electro-optic modulator in silicon technology,” *Opt. Express*, vol. 19, no. 12, pp. 11841–11851, Jun. 2011.
[128] J. D. Ryckman *et al.*, “Photothermal optical modulation of ultra-compact hybrid Si-VO_2 ring resonators,” *Opt. Express*, vol. 20, no. 12, pp. 13215–13225, Jun. 2012.
[129] F. J. Morin, “Oxides Which Show a Metal-to-Insulator Transition at the Neel Temperature,” *Phys. Rev. Lett.*, vol. 3, no. 1, pp. 34–36, Jul. 1959.
[130] M. F. Becker, A. B. Buckman, R. M. Walser, T. Lépine, P. Georges, and A. Brun, “Femtosecond laser excitation of the semiconductor-metal phase transition in VO2,” *Appl. Phys. Lett.*, vol. 65, no. 12, pp. 1507–1509, Sep. 1994.
[131] M. M. Qazilbash *et al.*, “Infrared spectroscopy and nano-imaging of the insulator-to-metal transition in vanadium dioxide,” *Phys. Rev. B*, vol. 79, no. 7, p. 075107, Feb. 2009.
[132] B. Wu, A. Zimmers, H. Aubin, R. Ghosh, Y. Liu, and R. Lopez, “Electric-field-driven phase transition in vanadium dioxide,” *Phys. Rev. B*, vol. 84, no. 24, p. 241410, Dec. 2011.
[133] C. N. Berglund and H. J. Guggenheim, “Electronic Properties of V${\mathrm{O}}_{2}$ near the Semiconductor-Metal Transition,” *Phys. Rev.*, vol. 185, no. 3, pp. 1022–1033, Sep. 1969.
[134] A. Cavalleri *et al.*, “Femtosecond Structural Dynamics in ${\mathrm{VO}}_{2}$ during an Ultrafast Solid-Solid Phase Transition,” *Phys. Rev. Lett.*, vol. 87, no. 23, p. 237401, Nov. 2001.
[135] M. Liu *et al.*, “Terahertz-field-induced insulator-to-metal transition in vanadium dioxide metamaterial,” *Nature*, vol. 487, no. 7407, pp. 345–348, Jul. 2012.
[136] J. Cao *et al.*, “Strain engineering and one-dimensional organization of metal-insulator domains in single-crystal vanadium dioxide beams,” *Nat. Nanotechnol.*, vol. 4, no. 11, pp. 732–737, Nov. 2009.
[137] G. Stefanovich, A. Pergament, and D. Stefanovich, “Electrical switching and Mott transition in VO 2,” *J. Phys. Condens. Matter*, vol. 12, no. 41, p. 8837, 2000.
[138] H. Wong and A. S. Helmy, “Performance Enhancement of Nano-Scale VO $_2$ Modulators using Hybrid Plasmonics,” *J. Light. Technol.*, vol. PP, pp. 1–1, Dec. 2017.
[139] H. W. Verleur, A. S. Barker, and C. N. Berglund, “Optical Properties of VO2 between 0.25 and 5 eV,” *Phys. Rev.*, vol. 172, pp. 788–798, Aug. 1968.
[140] “OSA | Nanoplasmonics: past, present, and glimpse into future.” [Online]. Available: https://www.osapublishing.org/oe/abstract.cfm?uri=oe-19-22-22029. [Accessed: 01-May-2018].
[141] J. A. Dionne, K. Diest, L. A. Sweatlock, and H. A. Atwater, “PlasMOStor: A Metal−Oxide−Si Field Effect Plasmonic Modulator,” *Nano Lett.*, vol. 9, no. 2, pp. 897–902, Feb. 2009.

[142] B. A. Kruger, A. Joushaghani, and J. K. S. Poon, “Design of electrically driven hybrid vanadium dioxide (VO_2) plasmonic switches,” *Opt. Express*, vol. 20, no. 21, pp. 23598–23609, Oct. 2012.
[143] S. Lysenko, A. Rua, F. Fernandez, and H. Liu, “Optical nonlinearity and structural dynamics of VO2 films,” *J. Appl. Phys.*, vol. 105, no. 4, p. 043502, Feb. 2009.
[144] Y. Zhou, X. Chen, C. Ko, Z. Yang, C. Mouli, and S. Ramanathan, “Voltage-Triggered Ultrafast Phase Transition in Vanadium Dioxide Switches,” *IEEE Electron Device Lett.*, vol. 34, no. 2, pp. 220–222, Feb. 2013.
[145] J. T. Kim, “CMOS-compatible hybrid plasmonic modulator based on vanadium dioxide insulator-metal phase transition,” *Opt. Lett.*, vol. 39, no. 13, pp. 3997–4000, Jul. 2014.

Copyright Acknowledgements

From: **AIPRights Permissions** Rights@aip.org
Subject: RE: permission for reusing a figure.1 from doi:10.1063/1.3653240
Date: March 14, 2018 at 10:29 PM
To: Mohamed Youssef Abdelatty el-jeo@aucegypt.edu

Dear Dr. Abdelatty:

Thank you for requesting permission to reproduce material from AIP Publishing publications.

Material to be reproduced:

Figure 1 from:
"Electro-absorption modulation in horizontal metal-insulator-siliconinsulator-metal nanoplasmonic slot waveguides"
APPLIED PHYSICS LETTERS. Doi:10.1063/1.3653240

For use in the following manner:

Reproduced in your thesis.

Permission is granted subject to these conditions:

1. AIP Publishing grants you non-exclusive world rights in all languages and media. This permission extends to all subsequent and future editions of the new work.

2. The following notice must appear with the material (please fill in the citation information):

"Reproduced from [FULL CITATION], with the permission of AIP Publishing."

When reusing figures, photographs, covers, or tables, the notice may appear in the caption or in a footnote.

In cases where the new publication is licensed under a Creative Commons license, the full notice as stated above must appear with the reproduced material.

3. If the material is published in electronic format, we ask that a link be created pointing back to the abstract of the article on the journal website using the article's DOI.

4. This permission does not apply to any materials credited to another source.

5. If you have not already done so, please attempt to obtain permission from at least one of the authors. The authors' contact information can usually be obtained from the article.

For future permission requests, we encourage you to use RightsLink, which is a tool that allows you to obtain permission quickly and easily online. To launch the RightsLink application, simply access the appropriate article on the journal site, click on the "Tools" link in the abstract, and select "Reprints & Permissions."

Please let us know if you have any questions.

Sincerely,
Susann Brailey

Manager, Rights & Permissions

AIP Publishing
1305 Walt Whitman Road | Suite 300 | Melville NY 11747-4300 | USA
t +1.516.576.2268
rights@aip.org | publishing.aip.org
Follow us: Facebook | Twitter | LinkedIn

From: Mohamed Youssef Abdelatty [mailto:el-jeo@aucegypt.edu]
Sent: Saturday, March 10, 2018 6:17 PM
To: AIPRights Permissions <Rights@aip.org>
Subject: permission for reusing a figure.1 from doi:10.1063/1.3653240

Dear Office of Rights and Permissions, AIP Publishing,

My name is Mohamed Youssef Abdelatty. I am a physics M.Sc. student at the AUC. By the end of this semester I am going to defend my M.Sc. degree. Right now, I am writing my thesis with the title: “Integrated Ultrafast Optical Modulators”.

I want to request a permission for reusing a figure.1 from “Electro-absorption modulation in horizontal metal-insulator-siliconinsulator-metal nanoplasmonic slot waveguides”. The authors of the paper are “Shiyang Zhu, G. Q. Lo, and D. L. Kwong”. The journal: APPLIED PHYSICS LETTERS. Doi:10.1063/1.3653240.

This permission will help me a lot towards getting my degree.

Regards,
Mohamed Y. Abdelatty
Graduate Student and Research Assistant
School of Science and Engineering
The American University in Cairo
Mob.: (+2) 01223424327
el-jeo@aucegypt.edu
mohamed.yousef@bue.edu.eg

Nano letters

ISSN:	1530-6992	**Language:**	English
Publication year(s):	2001 - present	**Country of publication:**	United States of America
Author/Editor:	American Chemical Society		
Publication type:	e-Journal		
Publisher:	AMERICAN CHEMICAL SOCIETY		
Rightsholder:	AMERICAN CHEMICAL SOCIETY		

Permission type selected: Republish or display content

Type of use selected: reuse in an Application/Technical Report

Select different permission

Article title: PlasMOStor: A Metal−Oxide−Si Field Effect Plasmonic Modulator
Author(s): Atwater, Harry A. ; et al
DOI: 10.1021/nl803868k
Date: Jan 26, 2009
Volume: 9
Issue: 2

Select different article

Terms and conditions apply to this permission type
View details

PERMISSION/LICENSE IS GRANTED FOR YOUR ORDER AT NO CHARGE

This type of permission/license, instead of the standard Terms & Conditions, is sent to you because no fee is being charged for your order. Please note the following:

- Permission is granted for your request in both print and electronic formats, and translations.
- If figures and/or tables were requested, they may be adapted or used in part.
- Please print this page for your records and send a copy of it to your publisher/graduate school.
- Appropriate credit for the requested material should be given as follows: "Reprinted (adapted) with permission from (COMPLETE REFERENCE CITATION). Copyright (YEAR) American Chemical Society." Insert appropriate information in place of the capitalized words.
- One-time permission is granted only for the use specified in your request. No additional uses are granted (such as derivative works or other editions). For any other uses, please submit a new request.

If credit is given to another source for the material you requested, permission must be obtained from that source.

Back

E-JOURNAL

ISSN:	1558-2213	**Language:**	English
Publication year(s):	2013 - present	**Country of publication:**	United States of America
Author/Editor:	Optical Society of America ; IEEE Lasers and Electro-optics Society		
Publisher:	IEEE]		
Rightsholder:	IEEE - INST OF ELECTRICAL AND ELECTRONICS ENGRS		

Academic

Photocopy or share content electronically

LICENSE COVERAGE

Annual Copyright License for Academic Institutions

This permission type is covered. The Annual Copyright License authorizes the licensee's faculty, staff, students, and other authorized users to distribute print and electronic copies of copyrighted content within your institution through:

- Print or electronic coursepacks
- Classroom handouts
- Electronic reserves
- Institution Intranets
- Course/Learning Management systems (CMS/LMS)
- CD-ROM/DVD
- Other internal academic uses

The description above is provided for summary purposes only. Please refer to your institution's Annual Copyright License for the complete terms and conditions and scope of coverage of the license.

Covered by CCC Annual License - Academic

E-JOURNAL

ISSN: 1557-1963
Language: English
Publication year(s): 2006 - present
Country of publication: United States of America
Publisher: Springer New York LLC

Rightsholder: SPRINGER SCIENCE & BUS MEDIA B V

Academic

Photocopy or share content electronically

LICENSE COVERAGE

Annual Copyright License for Academic Institutions

This permission type is covered. The Annual Copyright License authorizes the licensee's faculty, staff, students, and other authorized users to distribute print and electronic copies of copyrighted content within your institution through:

- Print or electronic coursepacks
- Classroom handouts
- Electronic reserves
- Institution Intranets
- Course/Learning Management systems (CMS/LMS)
- CD-ROM/DVD
- Other internal academic uses

The description above is provided for summary purposes only. Please refer to your institution's Annual Copyright License for the complete terms and conditions and scope of coverage of the license.

Covered by CCC Annual License - Academic

TERMS:

No more than 30% of this work may be used.

E-JOURNAL

ISSN:	1361-6463	**Language:**	English
Publication year(s):	1996 - present	**Country of publication:**	United Kingdom of Great Britain and Northern Ireland
Author/Editor:	Institute of Physics and the Physical Society ; Institute of Physics (Great Britain)		
Publisher:	IOP Publishing		
Rightsholder:	IOP PUBLISHING, LTD		

Academic

Photocopy or share content electronically

LICENSE COVERAGE

Annual Copyright License for Academic Institutions

This permission type is covered. The Annual Copyright License authorizes the licensee's faculty, staff, students, and other authorized users to distribute print and electronic copies of copyrighted content within your institution through:

- Print or electronic coursepacks
- Classroom handouts
- Electronic reserves
- Institution Intranets
- Course/Learning Management systems (CMS/LMS)
- CD-ROM/DVD
- Other internal academic uses

The description above is provided for summary purposes only. Please refer to your institution's Annual Copyright License for the complete terms and conditions and scope of coverage of the license.

Covered by CCC Annual License - Academic

From: **pubscopyright** copyright@osa.org
Subject: RE: permission for reusing a figure.1 from DOI:10.1364/OE.23.006878
Date: March 12, 2018 at 5:15 PM
To: Mohamed.Yousef Mohamed.Yousef@bue.edu.eg, pubscopyright copyright@osa.org

Dear Mohamed Y. Abdelatty,

Thank you for contacting The Optical Society.

For the use of figure 1 from Petr Markov, Kannatassen Appavoo, Richard F. Haglund, and Sharon M. Weiss, "Hybrid Si-VO2-Au optical modulator based on near-field plasmonic coupling," Opt. Express 23, 6878-6887 (2015):

> OSA considers your requested use of its copyrighted material to be Fair Use under United States Copyright Law. It is requested that a complete citation of the original material be included in any publication.

While your publisher should be able to provide additional guidance, OSA prefers the below citation formats:

> For citations in figure captions:
>
> [Reprinted/Adapted] with permission from ref [x], [Publisher]. (with full citation in reference list)
>
> For images without captions:
>
> Journal Vol. #, first page (year published) An example: Opt. Express 23, 6878 (2015)

OSA considers this email to be sufficient authorization for the use of the requested material.

Let me know if you have any questions.

Kind Regards,

Rebecca Robinson

Rebecca Robinson
March 12, 2018
Authorized Agent, The Optical Society

From: Mohamed.Yousef [mailto:Mohamed.Yousef@bue.edu.eg]
Sent: Sunday, March 11, 2018 2:58 PM
To: pubscopyright
Subject: permission for reusing a figure.1 from DOI:10.1364/OE.23.006878

Dear Office of Rights and Permissions, OSA Publishing,
My name is Mohamed Youssef Abdelatty. I am a physics M.Sc. student at the AUC. By the end of this semester I am going to defend my M.Sc. degree. Right now, I am writing my thesis with the title: "Integrated Ultrafast Optical Modulators".
I want to request a permission for reusing a figure.1 from "Hybrid Si-VO_2-Au optical modulator based on near-field plasmonic coupling". The authors of the paper are "Petr Markov, Kannatassen Appavoo, Richard F. Haglund, Jr. and Sharon M. Weiss1,2,4". The journal: OPTICS EXPRESS. DOI:10.1364/OE.23.006878.
This permission will help me a lot towards getting my degree.

Regards,
Mohamed Y. Abdelatty
Demonstrator
Basic Science Engineering
Room: 107 - Building: A
The British University in Egypt
Tel.: (+2 02) 26300013/4/5/6/7/8, Ext.: 2412
Mob.: (+2) 01223424327
mohamed.yousef@bue.edu.eg
el-jeo@aucegypt.edu